Title
Lateral Control of Heavy Vehicles for Automated Systems

Authors
Hingwe, Pushkar
Wang, Jen-Yu
Tai, Meihua
et al.

Publication Date
2003-03-01

CALIFORNIA PATH PROGRAM
INSTITUTE OF TRANSPORTATION STUDIES
UNIVERSITY OF CALIFORNIA, BERKELEY

Lateral Control of Heavy Vehicles for Automated Systems: Final Report for MOU 313

Pushkar Hingwe, Jen-Yu Wang, Meihua Tai, Masayoshi Tomizuka

California PATH Research Report
UCB-ITS-PRR-2003-10

This work was performed as part of the California PATH Program of the University of California, in cooperation with the State of California Business, Transportation, and Housing Agency, Department of Transportation; and the United States Department of Transportation, Federal Highway Administration.

Final Report for MOU 313

March 2003

ISSN 1055-1425

Lateral Control of Heavy Vehicles for Automated Highway Systems
Final Report for MOU 313

Pushkar Hingwe, Jeng-Yu Wang, Meihua Tai, Masayoshi Tomizuka* † ‡ §

March 21, 2003

*Pushkar Hingwe, pushkar@cal.berkeley.edu, formerly at California PATH is now at Hitachi, 0KB/28-2, 5600 Cottle Road, San Jose, CA 95193

†Jeng-Yu Wang, jwang@yahoo.com, is at Novellus Inc.

‡M. Tai, mtai@poly.duke.edu, is Assistant Prof. at Polytec University of New York

§Masayoshi Tomizuka, tomizuka@me.berkeley.edu, is Professor in the Department of Mechanical Engineering University of California Berkeley CA 94720

Contents

0.1 Executive Summary

This is the final report for MOU 313, "Lateral Control of Heavy Vehicles for Automated Highway Systems". It address the following task items: Analysis and synthesis of control algorithms based on system identification and calibration results (Task 4. in the MPU), Closed loop results at highway speeds (Task 5), limits and persormance of sensors, actuators and control schemes as infered from data collected during closed loop experiments at 55 MPH (task 6) and baseline safety requirements based on closed loop data (task 7)

Five controllers were designed based on the model identification study conducted on the previous phase of the project. This report will present the details of eash design methodology: Nonlinear Robust Loop Shaping, Robust controller based on Feedback linearization, Gain - Scheduled H_∞, Robust $H\infty$ and Linear Parameter Varying (LPV) controllers. The sysnthesis of each controller is sufficiently complex to merit a separate Chapter. These Chapters address Task 4 in detail.

Closed loop experiments were performed for Robust H_∞, nonlinear Sliding Mode Control (SMC) and LPV contorller. The results of these closed loop experiments will be presented in the Chapters that detail the control design respectively and address Task 5.

One of the control strategies, Linear Parameter Varying (LPV) was developed to address issues arising from variation in dynamics with the speed of the vehicle. Data collected from Robust H_∞ controller, which is designed for fixed speed, indicated that an LPV control strategy may work better for good steering control over a wide range of speeds. The gain scheduled H_∞ controller was also designed to address automated operation over a range of velocity.

The closed loop experiment results showed that the sensors (range, sensitivity and noise characteristics) on the experimental vehicle were adequate for effective automated steering at 55 MPH. Lateral deviation measurement sensors were adequate in range and sensitivity. Yaw rate and acceleration sensors were adequate for system identification but inadequate for effective implementation of nonlinear control strategies. Actuator performance was adequate (with bandwidth in excess of 10 Hz) for 400m step curvature change at 55 MPH. Performance of the closed loop controller as characterised by tracking accuracy at high speeds has been excellent. The LPV controller has been tested up to 70MPH. The limited length of track at Crow's Landing test site and large inertia of the truck semi-trailer vehicle posed limitations on testing the controllers to the "limit". However, the authors are pleased to report that the LPV controller provided smooth steering action with adequate tracking performance from start of the track under maximum possible acceleration to the end of track with aggressive deceleration (occasional brake locking). The curve transitions at Crow's Landing test site are aggressive and unlikely to exist at real highways. In that sense, the range of present sensors and performance of present controller and actuator was tested under limiting conditions and configuration on the test vehicle was deemed adequate. These conclusions addresses Task 6.

LPV model based controller emerged to be the right "supervisory controller" which combines information from longitudinal sensor (velocity) and imposes restriction on the longitudinal controller in terms of maximum allowed deceleration and maximum allowed aceleration. This addresses Task 7 of MOU 313.

A video of the controllers was taken at the Crow's Landing test site and is available at PATH Publications office and on the PATH web site. A copy is included with this report.

Report is organized in Chapters. First two Chapters presents Nonlinear Controllers which have sound robustness properties but are sensitive to sensor noise. Subsequent Chapters present Robust H_∞ contoller and Gain Scheduled Controller. Finally the last Chapter will propose LPV controller as a method to combine the benefits of converting the vehicle model nonlinear

in velocity to a linear time varying model with velocity as the measured parameter and utilizing rich tool set of Linear H_∞ based control design. Each Chapter is self sufficient in content. This allows reader to read Chapters in any order or preference. Conclusions presented in the last Chapter tie the lessons from each different controller.

Chapter 1

Introduction

Automated operation of vehicles on highways has been proposed to increase throughput, safety and fule economy. In the context of Intelligent Transportation Systems (ITS), Automated Highway Systems (AHS) and Advanced Vehicle Control Systems (AVCS) the importance of heavy vehicles is pronounced. Profit oriented operation of heavy vehicles makes their study in the context of ITS, AHS and AVCS commercially important. Apart from cost benefits, AVCS technologies have a strong potential to improve safety of heavy vehicle traffic by reducing driving stress on the driver. This has attracted attention of the automobile industry and the academic research community (Chen and Tomizuka 1995, Canudas 1998, Fritz 1999, Bruin et al. 1999, Kanellakopoulos 1999, Stepanapoulou 2000).

The California PATH (Partners for Advanced Transit and Highways) has been playing a leading role in the research of AHS for more than a decade. Automatic lane guidance or lateral control is an important aspect of automating the heavy vehicle operation. Therefore, the automated steering for lane guidance of heavy vehicles for AHS is one of the main research focusesin California PATH[17].

Design of a lane guidance controller involves determination of the steering input that trades off best the following usual control objectives: tracking performance (how centered the vehicle is in the lane), passenger comfort (smooth lateral motion), steering action (bandwidth issue) and robustness (parameters and environment).

The challenges arise in controlling heavy vehicle lateral dynamics are:
(i) Large inertia which causes slower response to steering.
(ii) Inherent nonlinearities in the vehicle model such as the longitudinal velocity (when it is considered an independent state of the model) and tire lateral force saturation.
(iii) Unusually large uncertainties in vehicle parameters and environmental disturbances.

Chen and Tomizuka [29] developed a control model of single-unit HDV (tractor-semitrailer type) for AHS and designed a nonlinear steering and braking controller using the input-output linearization in [1]. The specific models used or derived in this report are largly based on this initial effort. They also proposed a back-stepping based algorithm for automatic steering and brake control of tractor semi-trailers[1].

During the execution of MOU 313, several lateral control algorithms were developed and tested either in simulation or on the tractor semi-trailer vehicle donated by Freightliner Corp. The previous report of the project covered in detail the hardware set up of the experimental vehilces, subsystem loop designs (e.g. the steering loop) and some control design methodologies such as loop shaping controller and SMC controller.

This report will present the closed loop results achieved at high speeds (greater than 55MPH) and control methodologies which address robustness and vehicle nonlinearities.

Specifically, the report will address the following task items

- Task 4. Analysis and synthesis of control algorithms based on system identification and calibration results.
- Task 5. Closed loop results
- Task 6. Limits and persormance of sensors, actuators and control schemes as infered from data collected during closed loop experiments at 55 MPH
- Task 7. Baseline safety requirements based on closed loop data

Five controllers were designed to address the above tasks. This report will present the details of eash design methodology: Nonlinear Robust Loop Shaping, Robust controller based on Feedback linearization, Gain -Scheduled H_∞, Robust $H\infty$ and Linear Parameter Varying (LPV) controllers. The sysnthesis of each controller is sufficiently complex to merit a separate Chapter. These Chapters address Task 4 in detail.

Closed loop experiments were performed for Robust H_∞, nonlinear Sliding Mode Control (SMC) and LPV contorller. The results of these closed loop experiments will be presented in the Chapters that detail the control design respectively and address Task 5.

One of the control strategies, Linear Parameter Varying (LPV) was developed to address issues arising from variation in dynamics with the speed of the vehicle. Data collected from Robust H_∞ controller, which is designed for fixed speed, indicated that an LPV control strategy may work better for good steering control over a wide range of speeds. The gain scheduled H_∞ controller was also designed to address automated operation over a range of velocity.

The closed loop experiment results showed that the sensors (range, sensitivity and noise characteristics) on the experimental vehicle were adequate for effective automated steering at 55 MPH. Lateral deviation measurement sensors were adequate in range and sensitivity. Yaw rate and acceleration sensors were adequate for system identification but inadequate for effective implementation of nonlinear control strategies. Actuator performance was adequate (with bandwidth in excess of 10 Hz) for 400m step curvature change at 55 MPH. Performance of the closed loop controller as characterised by tracking accuracy at high speeds has been excellent. The LPV controller has been tested upto 70MPH. The limited length of track at Crow's Landing test site and large inertia of the truck semi-trailer vehicle posed limitations on testing the controllers to the "limit". However, the authors are pleased to report that the LPV controller provided smooth steering action with adequate tracking performance from start of the track under maximum possible acceleration to the end of track with aggressive deceleration (occasional brake locking). The curve transitions at Crow's Landing test site are aggressive and unlikely to exist at real highways. In that sense, the range of present sensors and performance of present controller and actuator was tested under limiting conditions and configuration on the test vehicle was deemed adequate. These conclusions addresses Task 6.

LPV model based controller emerged to be the right "supervisory controller" which combines information from longitudinal sensor (velocity) and imposes restriction on the longitudinal controller in terms of maximum allowed deceleration and maximum allowed aceleration. This addresses Task 7 of MOU 313

A video of the controllers was taken on Crow's Landing and is available at PATH Publications office and on the PATH web site. A copy is included with this report.

The report is organized into five Chapters presenting details of each control methodoligy in terms of motivation, synthesis and impact on the performance, robustness of the closed loop system.

The model of the tractor semitrailer is nonlinear and therefore nonlinear design methodologies were considered for steering control.

Chapter 2 presents nonlinear loop shaping controller based on Sliding Mode Control (SMC). The steering dynamics are explicitly used in control synthesis. input pre-filtering is used to prevent control chatter and saturation. SMC controller was tested on the experimental vehicle in closed loop.

Chapter 3 presents nonlinear controllers based on robust feedback linearization approach and compares them to SMC based approach.

The nonlinear controllers, while addressing robustness explicitly, do not address measurement noise. Smoothness of steering control is also a conflicting performance objective to nonlinear control strategies such as SMC which require fast switching of the steering control.

Linear optimal control methodologies address robustness and performance in presence of sensor noise but require that the vehicle operate in a linear fashion. On a highway at slowly varying speeds and small steering angles, the linear approximation of vehicle dynamics is valid. Thus several linear control strategies were explored. The details of these designs are presented in subsequent chapters.

Chapter 4 presents linear controller based on H_∞ optimization. By choosing frequency based weighting filters, the smoothness of steering effort is achieved. Simulations show that the tracking performance is also achieved. This controller was tested in closed loop and performned well for designed velocity range.

Vehicle longitudinal velocity makes the linear model of the vehicle time varient and Liner Time Invarient (LTI) design methodologies do not guarantee robustness or performance. Designing linear controllers as a function of velocity is one possible way to address this issue. The remaining chapters were developed with this view.

Chapter 5 presents linear gain scheduled controller to address optimality and stability of controller in face of variation in longitudinal velocity. The designed controller is shown stable for a range of longitudinal speeds by simulation.

Chapter 6 Presents Linera Parameter Varying controller for steering control. Unlike Gain Scheduling which switches between controllers, the controller designed using LPV technique is a single controller expressed as a function of the velocity. (The implementation of the controller, however, demands discretization with respect to velocity because of computational cost reasons). This controller worked well for velocities exceeding 55MPH on Crow's Landing test track.

Chapter 2

Nonlinear Robust Loop Shaping Controller

A new nonlinear robust controller design method is proposed for the lateral control of heavy vehicles for the automated highway systems. In the controller design, the actuator dynamics is explicitly taken into account. A first order pre-filter is introduced to reduce chattering which is inherent in the nonlinear robust controller and to prevent the saturation in the front wheel steering angle and steering system slew rate. Constructive backstepping design technique is utilized in the design of robust controller for the augmented system . Simulation results are shown.

Keywords: Nonlinear control, robust control, backstepping design, Automated Highway Systems, lateral control, heavy vehicles

2.1 Introduction

Heavy vehicles are very important components in transportation systems and they are gaining increasing interest among the Automated Highway Systems (AHS) research community. The California PATH (Partners for Advanced Transit and Highways) has been playing a leading role in the research of AHS, and recently, the automated steering for lane guidance of heavy vehicles for AHS is one of its main research focuses[17].

Heavy vehicles exhibit much more complex dynamical characteristics compared to the passenger cars. For example, the tractor-semitrailer combination has two units connected by the fifth wheel and because of that, the roll and pitch motions of the tractor and semitrailer are coupled. The external forces to the vehicle system come from the interactions between tires and road. The tire forces are very complicated functions of many parameters such as road adhesion coefficient, tire velocity and tire vertical force. In the heavy vehicles, because of the higher center of gravity, the load transfer effect is more significant than in the passenger cars. Moreover, different cargo and different loading configuration exert different force on each tire of the heavy vehicle. All of these motivate the design of controllers working directly on nonlinear models and imply that robust control schemes have to be used to assure the stability of the closed automated steering control system in the presence of model uncertainties.

Chen and Tomizuka proposed to use differential braking forces of the semitrailer along with the front wheel steering in the lateral lane guidance of heavy vehicles[1]. The use of the dif-

ferential braking forces prevent potential occurrences of undesirable phenomena such as trailer swing and jack-kniffing. They assumed a perfect nonlinear model of the vehicle system and used backstepping technique in the controller design. Tai and Tomizuka designed a Sliding Mode Controller (SMC) explicitly taking the model uncertainties into considerations. In SMC, the larger the model uncertainty, the higher the control gain. In the heavy vehicle model, there exist both parametric uncertainties and unmodeled dynamics[18]. Tai and Tomizuka also proposed the use of Adaptive Robust Control (ARC) for lateral control of heavy vehicles[18]. ARC incorporates the adaptive control technique to the design of robust control such as SMC while overcoming the drawbacks of the adaptive control and remedies the high gain nature of the SMC. Ackermann, et al. introduced an integrator at the output of the vehicle control system to guarantee the static robust performance while reducing chattering problem when the saturation function is used in the SMC[19]. On the other hand, Hingwe and Tomizuka designed a SMC controller by introducing an integrator at the input of the vehicle control system to reduce the chattering of the control input[20].

In the above mentioned controller designs, the control input is the front wheel steering angle and the dynamics of the steering subsystem was not considered. In actual systems, there are physical limits both in the steering angle and the steering rate. On a test vehicle, Freightliner tractor-semitrailer, a steering actuator (DC motor and its current control unit) is installed. In our lateral vehicle control architecture, an inner loop controller is designed to let the front steering wheel follow the desired steering angle calculated by vehicle lateral control loop, outer loop. In this chapter, we model the closed steering subsystem as a first order dynamical system with model uncertainty. To prevent the actuator saturation and reduce chattering while explicitly taking into account the vehicle model uncertainty and actuator model uncertaintly in the controller design, the vehicle system is extended with a first order pre-filter at the input side of the steering actuator. The added pre-filter will also filter sensor noise. The input to the augmented system is the input to the pre-filter and because the model uncertainties are not in the same channel as in the control input, the robust sliding mode control technique can not be directly applied. We apply the constructive backstepping method[21] to the extended system, and the input to the steering actuator is the output of the pre-filter.

2.2 System Model Description

2.2.1 Model in Unsprung Mass Coordinate System

The simplified control model of tractor-semitrailer heavy vehicles has 3 degrees of freedom: tractor lateral motion, tractor yaw motion and yaw motion of the semitrailer relative to the tractor. The road-vehicle interaction is represented by linear functions of tire slip angles. The simplified model used in the controller design throughout this chapter is derived using the method proposed in[22] by setting the number of units equal to 2. The tractor-semitrailer and its dimensions are shown in Fig. 2.1.

Let the generalized coordinate be $\dot{q} = [V_y, \dot{\epsilon}_1, \dot{\epsilon}_f]$, where V_y is the lateral velocity of the tractor, $\dot{\epsilon}_1$ and $\dot{\epsilon}_f$ are the tractor yaw rate and the trailer relative yaw rate respectively. Then, the simplified vehicle model with respect to the unsprung mass frame of the tractor is

$$M\ddot{q} + C(q, \dot{q}) = 2C_{\alpha f}[1, l_f, 0]^T \delta_f \tag{2.1}$$

where δ_f is the front wheel steering angle, M is a 3×3 inertia matrix and C is a 3×1 vector whose elements are functions of q, $\dot{q}$ and other vehicle parameters.

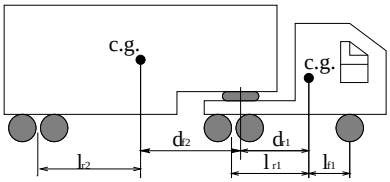

Figure 2.1: Tractor-Semitrailer

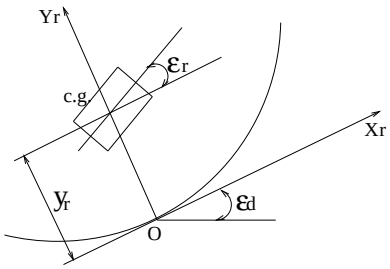

Figure 2.2: Virtual Look-ahead Distance

2.2.2 Model in the Road Coordinate System and Virtual Look-ahead Distance

In vehicle lateral control, the control objective is to let the vehicle's center of gravity follow the road center line on highways, while guaranteeing ride comfort. The tracking error has to be physically measured or calculated with respect to the road center line, and the position and the relative orientation of the vehicle with respect to the road need to be given explicitly. Thus the road reference $O_rX_rY_r$ in Fig.2.2 is introduced[22].

The tractor-semitrailer model in the road coordinate system is given by

$$M_1\ddot{q}_r + C_1(q_r, \dot{q}_r) + D_1\dot{\epsilon}_d(t) + E_1\epsilon_d(t) = F_1\delta_f \tag{2.2}$$

where $q_r = [y_r, \epsilon_r, \epsilon_f]^T$, y_r is the lateral error at the tractor's center of gravity (C.G.), ϵ_r is the tractor yaw error relative to the road center line, ϵ_f is the articulation angle, and ϵ_d and $\dot{\epsilon_d}$ are desired yaw angle and desired yaw rate respectively. Here, it is assumed that $\ddot{\epsilon}_d = 0$, i.e., the highways are smooth connections of straight sections and arcs with constant road curvatures.

The lateral error(y_v) at any distance d_v(virtual look-ahead distance) from the C.G. can be synthesized as

$$y_v = y_r + d_v\epsilon_r \tag{2.3}$$

and it is used for feedback control. In order to keep the tractor's C.G. follow the road center line, the virtual sensor should follow a trajectory, $y_{s,desire}$, instead of the road center line. In this Chapter, the desired trajectory is given by

$$y_{v,desire} = d_v\bar{\epsilon}_r \tag{2.4}$$

where $\bar{\epsilon}_r$ is the steady state yaw error, which depends on the vehicle speed and the road curvature ($\bar{\epsilon}_r = 0$ on straight roads).

2.2.3 Steering System Dynamics

The steering system is a critical component of the vehicle lateral control system. From the viewpoint of vehicle lateral control, the front wheel steering angle is often regarded as the control input. The actual control input, however, is the command signal to the actuator, which is set by the lateral controller. Thus, the dynamics of the steering system must be considered along with the vehicle lateral dynamics in the design of vehicle lateral control system.

Research on heavy vehicles by California PATH uses a Freightliner FLD 120 truck as an experimental test vehicle. The existing steering system on the Freightliner truck has been retrofitted with an electric steering actuator mounted directly on the steering column of the existing steering system. Then, an inner loop controller is designed for the steering subsystem to let the steering wheel track the desired trajectory set by the vehicle lateral controller[23]. The steering system has a physical limit in the steering angle and the steering actuator has a limit in the slew rate. With the inner loop controller, the closed loop steering system is modeled as a first order linear system with unmodeled dynamics.

$$\dot{\delta}_f = \frac{1}{\tau_a}(\delta_a - \delta_f) + \Delta(\delta_f, q_r) \tag{2.5}$$

where δ_a is the input to the steering actuator and τ_a is the time constant.

2.2.4 Lateral Control Model of Tractor-semitrailer System

To prevent the actuator saturation and reduce chattering while explicitly taking into account the vehicle model uncertainty and actuator model uncertaintly in the controller design, the vehicle dynamics is augmented with a first order prefilter at the input side of the steering actuator.

$$\delta_a(S) = \frac{1}{\tau_1 S+1} u(S) \tag{2.6}$$

From Eqs. (2.1), (2.2), (2.3), (2.5) and (2.6), the lateral control model of the tractor-semitrailer system with steering system dynamics and prefilter can be written as

$$\begin{array}{rcl} \dot{x} & = & b_{x0}(x)\delta_f + f_{x0}(x) + \tilde{f}_{x2}(x) \\ \ddot{y}_v & = & b_0(x)\delta_f + f_0(x) + \tilde{f}_2(x,t) \\ \dot{\delta}_f & = & \frac{1}{\tau_a}(\delta_a - \delta_f) + \Delta(x, \delta_f) \\ \dot{\delta}_a & = & \frac{1}{\tau_1}(u - \delta_a) \end{array} \tag{2.7}$$

In the above system, x is the state variable ($x = [y_r, \dot{y}_r, \epsilon_r, \dot{\epsilon}_r, \epsilon_f, \dot{\epsilon}_f]^T$), $b_{x0}(x), f_{x0}(x), b_0(x)$ and $f_0(x)$ are known functions, and $\tilde{f}_{x2}(x), \tilde{f}_2(x,t)$ and $\Delta(x, \delta_f)$ are functions used to represent all terms that cannot not be modeled exactly. In the subsequent sections, controllers will be designed based on (2.7). Considering the physical properties of the system, the following reasonable assumptions are made.

Assumption 1 *The unknown nonlinear functions are bounded above by known functions, i.e.,*

$$\begin{array}{l} \|\tilde{f}_2\| \le \beta_1(x) \\ \|\tilde{f}_{x2}\| \le \beta_{x1}(x) \\ \|\Delta\| \le \beta_2(x, \delta_f) \end{array} \tag{2.8}$$

where $\beta_1(x) \in C^3(x)$, $\beta_{x1}(x) \in C^3(x)$ and $\beta_2(x, \delta_f) \in C^3(x, \delta_f)$ are known functions $\diamondsuit$

Assumption 2 *$b_0(x)$ and $b_{x0}(x)$ are positive functions.*

Note that the first assumption is about the extent of model uncertainties. The second assumption is to ensure that the input gain for the first two equations of (2.7) are nonzero all the time. *The objective is to design a control law for u such that the output y_v will track the desired output trajectory $y_d(t)$ as close as possible* . Since the model uncertainties, $\tilde{f}_{x2}, \tilde{f}_2$ and Δ, do not satisfy the matching condition, we use the backstepping method.

2.3 Robust Controller Design

The lateral position at the virtual sensor location (y_v) has relative degree of two with respect to the front wheel steering angle (δ_f). Let the sliding variable* be defined as

$$S = \dot{e} + \lambda e \tag{2.9}$$

where $e = y_v - y_{v,desire}$ is the output tracking error and λ is a positive constant. To avoid large input when the initial tracking error $e(0)$ is large, a modified sliding variable is defined as

$$\bar{S} = S + S(0)exp(-\lambda_1 t) \tag{2.10}$$

where λ_1 is a positive number. Define

$$\tilde{\delta}_f(x, \delta_f) = \delta_f - \alpha_1(x, t) \tag{2.11}$$

where, $\alpha_1(x,t)$ is the desired front wheel steering angle which will be synthesized later. From Eq.(2.7),

$$\begin{aligned} \dot{\bar{S}} &= b_0(x)\delta_f + f_0(x) + \tilde{f}_2(x,t) - \ddot{y}_{v,desire} \\ &\quad +\lambda\dot{e} + \lambda_1 S(0)exp(-\lambda_1 t) \\ &= b_0(x)\alpha_1(x) + f_0(x) - \ddot{y}_{v,desire} + \lambda\dot{e} \\ &\quad +\lambda_1 S(0)exp(-\lambda_1 t) + \tilde{f}_2(x,t) + b_0(x)\tilde{\delta}_f(x,\delta_f) \end{aligned} \tag{2.12}$$

Choose $\alpha_1(x,t)$ as

$$\begin{aligned} \alpha_1(x,t) &= -\tfrac{1}{b_0(x)}(f_0(x) - \ddot{y}_{v,desire} + \lambda\dot{e} \\ &\quad +\lambda_1 S(0)exp(-\lambda_1 t) + (c_1 + \tfrac{\beta_1^2}{4\epsilon_1})\bar{S}) \end{aligned} \tag{2.13}$$

where c_1 and ϵ_1 are positive constants. Define the candidate Lyapunove function

$$V_1 = \tfrac{1}{2}\bar{S}^2 \tag{2.14}$$

Then, from Eqs. (2.11), (2.12), (2.13) and (2.14), we have

$$\begin{aligned} \dot{V}_1 &= \bar{S}\dot{\bar{S}} \\ &\leq -c_1\bar{S}^2 + \tilde{f}_2\bar{S} - \tfrac{\beta_1^2}{4\epsilon_1}\bar{S}^2 + b_0\bar{S}\tilde{\delta}_f \\ &\leq -c_1\bar{S}^2 + \epsilon_1 + b_0\bar{S}\tilde{\delta}_f \end{aligned} \tag{2.15}$$

*S is called the sliding variable although the exact sliding is not attempted in this chapter in order to avoid chattering. For example, Eq.(2.13) involves a term proportional to S instead of a signum function of S

which means that if $\tilde{\delta}_f = 0$, i.e. the output of the steering system tracks the desired front wheel steering angle (α_1) exactly, then the sliding variable will asymptotically converg to a ball, whose size is defined by ϵ_1. From Eq. (2.13),

$$\begin{aligned} \dot{\alpha}_1 &= \frac{\partial \alpha_1}{\partial x}\dot{x} + \frac{\partial \alpha_1}{\partial t} \\ &= \hat{\dot{\alpha}}_1 + \tilde{\dot{\alpha}}_1 \end{aligned} \tag{2.16}$$

where $\hat{\dot{\alpha}}_1$ and $\tilde{\dot{\alpha}}_1$ are given by

$$\begin{aligned} \hat{\dot{\alpha}}_1 &= \frac{\partial \alpha_1}{\partial x}(f_{x0} + b_{x0}\delta_f) + \frac{\partial \alpha_1}{\partial t} \\ \tilde{\dot{\alpha}}_1 &= \frac{\partial \alpha_1}{\partial x}\tilde{f}_{x2} \end{aligned} \tag{2.17}$$

Modify the Lyapunov function candidate V_1 to

$$V_2 = V_1 + \frac{1}{2\Gamma_1}\tilde{\delta}_f^2 \tag{2.18}$$

where Γ_1 is a positive control parameter. Then,

$$\begin{aligned} \dot{V}_2 &= \dot{V}_1 + \frac{1}{\Gamma_1}\tilde{\delta}_f\dot{\tilde{\delta}}_f \\ &\leq -c_1\bar{S}^2 + \epsilon_1 + b_0\bar{S}\tilde{\delta}_f \\ &\quad + \frac{1}{\Gamma_1}\tilde{\delta}_f(\frac{1}{\tau_a}(\delta_a - \delta_f) + \Delta - \hat{\dot{\alpha}}_1 - \tilde{\dot{\alpha}}_1) \\ &\leq -c_1\bar{S}^2 + \epsilon_1 \\ &\quad + \frac{1}{\Gamma_1}\tilde{\delta}_f(\Gamma_1 b_0\bar{S} + \frac{1}{\tau_a}(\delta_a - \delta_f) + \Delta - \hat{\dot{\alpha}}_1 - \tilde{\dot{\alpha}}_1) \end{aligned} \tag{2.19}$$

Define the desired input to the steering actuator by

$$\alpha_2 = \delta_f - \tau_a(\Gamma_1 b_0\bar{S} - \hat{\dot{\alpha}}_1 + \Gamma_1(c_2 + \frac{\beta_3^2}{4\epsilon_2})\tilde{\delta}_f) \tag{2.20}$$

where c_2 and ϵ_3 are positive control parameters and $\beta_3(x, \delta_f, t)$ is a know function satisfying

$$|\frac{1}{\Gamma_1}(\Delta - \tilde{\dot{\alpha}}_1)| \leq \beta_3(x, \delta_f, t) \tag{2.21}$$

Define

$$\tilde{\delta}_a = \delta_a - \alpha_2 \tag{2.22}$$

then, from Eqs. (2.19), (2.20) and (2.22)

$$\begin{aligned} \dot{V}_2 &\leq -c_1\bar{S}^2 + \epsilon_1 - c_2\tilde{\delta_f}^2 \\ &\quad + \frac{1}{\Gamma_1}(\tilde{\dot{\alpha}}_1 + \Delta)\tilde{\delta}_f - \frac{\beta_3^2}{4\epsilon_2}\tilde{\delta}_f^2 + \frac{1}{\Gamma_1}\tilde{\delta}_f\frac{\tilde{\delta}_a}{\tau_a} \\ &\leq -c_1\bar{S}^2 + \epsilon_1 - c_2\tilde{\delta_f}^2 + \epsilon_2 + \frac{1}{\Gamma_1}\tilde{\delta}_f\frac{\tilde{\delta}_a}{\tau_a} \end{aligned} \tag{2.23}$$

From Eq.(2.20),

$$\begin{aligned} \dot{\alpha}_2 &= \frac{\partial \alpha_2}{\partial x}\dot{x} + \frac{\partial \alpha_2}{\partial \delta_f}\dot{\delta}_f + \frac{\partial \alpha_2}{\partial t} \\ &= \hat{\dot{\alpha}}_2 + \tilde{\dot{\alpha}}_2 \end{aligned} \tag{2.24}$$

where

$$\begin{aligned} \hat{\dot{\alpha}}_2 &= \frac{\partial \alpha_2}{\partial x}(b_{x0}\delta_f + f_{x0}) + \frac{\partial \alpha_2}{\partial \delta_f}\frac{\delta_a - \delta_f}{\tau_a} + \frac{\partial \alpha_2}{\partial t} \\ \tilde{\dot{\alpha}}_2 &= \frac{\partial \alpha_2}{\partial x}\tilde{f}_{x2} + \frac{\partial \alpha_2}{\partial \delta_f}\Delta \end{aligned} \tag{2.25}$$

Now, we design the control input u such that the input to the steering actuator follows α_2. Define the candidate Lyapunov function

$$V = V_2 + \frac{1}{2\Gamma_2}\tilde{\delta}_a^2 \tag{2.26}$$

where Γ_2 is a positive control parameter. Then,

$$\begin{aligned} \dot{V} &= \dot{V}_2 + \frac{1}{\Gamma_2}\tilde{\delta}_a\dot{\tilde{\delta}}_a \\ &= -c_1\bar{S}^2 + \epsilon_1 - c_2\tilde{\delta}^2 + \epsilon_2 + \frac{1}{\Gamma_1\tau_a}\tilde{\delta}_f\tilde{\delta}_a \\ &\quad + \frac{1}{\Gamma_2}\tilde{\delta}_a(\frac{1}{\tau_1}(u-\delta_a) - \dot{\hat{\alpha}}_2 - \dot{\tilde{\alpha}}_2) \\ &= -c_1\bar{S}^2 + \epsilon_1 - c_2\tilde{\delta}^2 + \epsilon_2 \\ &\quad + \frac{1}{\Gamma_2}\tilde{\delta}_a(\frac{\Gamma_2}{\Gamma_1\tau_a}\tilde{\delta}_f + \frac{1}{\tau_1}(u-\delta_a) - \dot{\hat{\alpha}}_2 - \dot{\tilde{\alpha}}_2) \end{aligned} \tag{2.27}$$

Choose u as

$$u = \delta_a - \tau_1(\frac{\Gamma_2}{\Gamma_1}\tilde{\delta}_f\frac{1}{\tau_a} - \dot{\hat{\alpha}}_2 + \Gamma_2(c_3 + \frac{\beta_4^2}{4\epsilon_3})\tilde{\delta}_a) \tag{2.28}$$

where c_3 and ϵ_3 are positive constants and $\beta_4(x, \delta_f, \delta_a, t)$ is a known function satisfying

$$|\dot{\tilde{\alpha}}_2\tilde{\delta}_a| \leq \beta_4(x, \delta_f, \delta_a, t) \tag{2.29}$$

From Eqs.(2.27) and (2.28), we finally have

$$\dot{V} = -c_1\bar{S}^2 + \epsilon_1 - c_2\tilde{\delta}_f^2 + \epsilon_2 - c_3\tilde{\delta}_a^2 + \epsilon_3 \tag{2.30}$$

The following theorem can readily be proved using above arguments.

Theorem 1 *If the internal dynamics of the system given by Eq. (2.7) is stable, then the robust backstepping control law (2.28) guarantees that the resulting closed-loop system is globally stable and the output tracking error e will converge to a ball, whose size depends on ϵ_1, ϵ_2 and ϵ_3.*

2.4 Simulation Results

We have simulated two controllers for two different plants under different road conditions and results are shown in Figs. 2.3, 2.4 and 2.5. Controller-A is a controller designed without explicitly taking into account the steering actuator dynamics, i.e., α_1 given by Eq.(2.13) is considered to be the steering input, δ_f. Controller-B is the controller proposed in this chapter which included the steering actuator dynamics in the system model and extend it with a first order filter. Two plants we considered are: Plant-A, without actuator dynamics, and Plant-B, with first order actuator dynamics. Figures 2.3 and 2.4 show the simulation results when the vehicle model has only unmodeled dynamics and no parametric uncertaities. Figure 2.5 shows the simulation results of the vehicle model with 30% of parametric uncertainty in the tire cornering stiffness in addition to the unmodeled dynamics. Each figure shows, from left-upper plot to right-bottom plot, front wheel steering angle, tractor yaw error relative to the road, lateral error at the center of gravity, lateral acceleration of the tractor, articulation angle and trator yaw rate.

As we can see from the simulation results, when Controller-A applied to Plant-B(actual system) it has severe oscillations (dashed line in Fig. 2.3, $c_1 = 4.0$); as we decrease the controller gain (c_1), the oscillation mode becomes less severe, but, the magnitude of the front wheel steering angle becomes larger (dashdotted($c_1 = 8.0$) and dashed ($c_1 = 20.0$) lines in Fig. 2.4). On the other hand, Controller-B (solid line in Fig.2.4) provides smoother response and smaller front

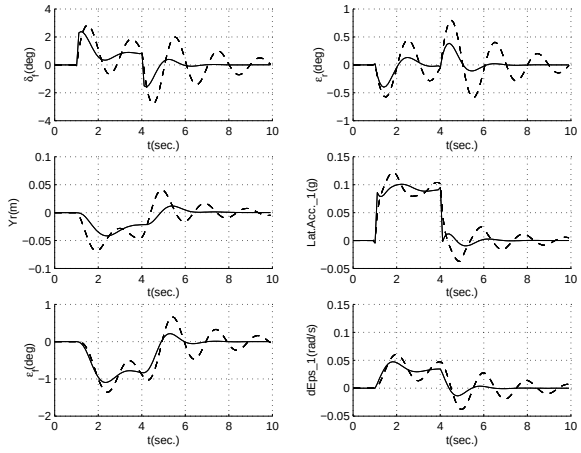

Figure 2.3: Simulation results-1

wheel steering angle. When there are parametric uncertainties in the tire cornering stiffness(Fig. 2.5), similar phenomena show up as in the case of unmodeled dynamics only. In Fig. 2.5, dotted line represents the simulation results of Contorller-B; solid, dashed and dashdotted lines represents the simulation results of Controller-A with the feedback gain(c_1) in the increasing order. The larger the size of the model uncertainties, the higher the resulting control gain of the traditional robust controller designed methods such as SMC[18]. Accordingly, in the case of larger model uncertainties, the effective control gain reduction and assurance of stability and riding comfort(smoothness) is more imperative. Note that Controller-B has larger tracking error than Controller-A in each simulation scenarios, though they are all within the acceptable limit ($0.2m$).

2.5 Conclusion

In this Chapter, the steering system dynamics was considered in the design of lateral control of heavy vehicles. To reduce chattering and prevent saturation in the front wheel steering angle and steering rate, a first order pre-filter was introduced to the input side of the steering actuator and then a robust controller was designed utilizing backstepping method. Simulation results showed the effectiveness of the proposed controller in neutralizing the high control gain nature of robust controllers and improving closed loop performance.

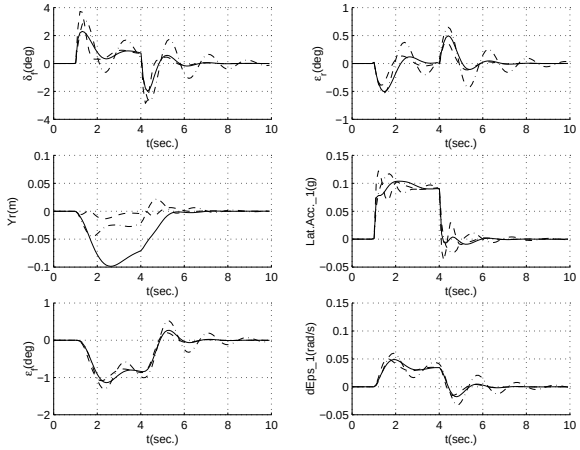

Figure 2.4: Simulation results-2

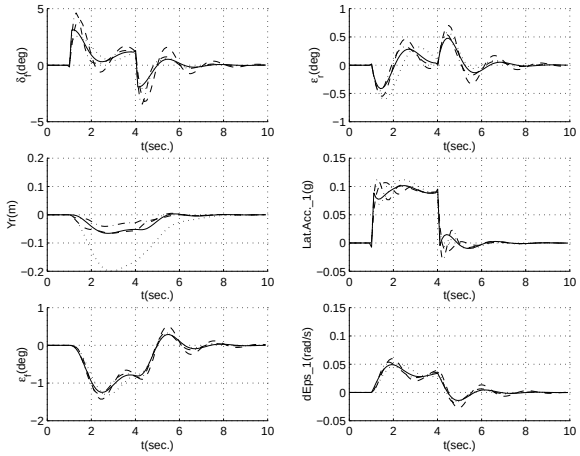

Figure 2.5: Simulation results-3

Chapter 3

Robust Controllers Based on Feedback Linearization

The first part of this chapter considers the design of nonlinear lateral controllers for tractor-semitrailer vehicles on automated highway systems. Two different but closely related design approaches are presented. One design proceeds along the line of uniformly ultimate bounded control, and the other along the line of sliding mode control. In either approach, the idea of feedback linearization is utilized to deal with nominal nonlinear dynamics of the tractor-semitrailer vehicles. Uncertain dynamics are treated differently in two approaches. The second part examines the two approaches and other robust control approaches including linear robust controllers from the viewpoint of implementation such as tuning controller parameters for performance, sensor requirement, and the complexity of real time control algorithms.

Keywords: Nonlinear control, robust control, automated highway systems, lateral control, heavy vehicles

3.1 Introduction

The idea of Automated Highway Systems (AHS) is an attractive option in solving the ever-growing need of increasing traffic throughput/capacity and relieving congestion. Lateral control of vehicles in the light of Intelligent Vehicle Highway Systems (IVHS) and AHS has long been an active research subject. In the past, the automated vehicle control for AHS has mostly been on passenger vehicles (Fenton et al., 1991, Shladover et al., 1991). Heavy vehicles are very important components of transportation systems and they are gaining increasing interest among the AHS research community. The California PATH (Partners for Advanced Transit and Highways) has been playing a leading role in the research of AHS, and recently, the study of the automated lane guidance of heavy vehicles for AHS is one of its main research focuses.

This chapter is concerned with the lateral guidance of heavy vehicles. Two major control objectives in the vehicle lateral control are to maintain small lateral errors and to ensure passenger comfort. The dynamics of the heavy vehicles are highly nonlinear and very involved. Vehicle models used in the controller design have unmodeled dynamics and parametric uncertainties (Tai and Tomizuka, 1999). All of these motivate nonlinear robust control approaches being utilized to assure the stability of the closed automated steering control system in the presence of the model uncertainties while proving riding comfort.

There are some works reported on the design of nonlinear controllers for automated lane guidance of heavy vehicles. Chen and Tomizuka (1995) utilized adaptive backstepping method and proposed simultaneous steering and differential braking control for tractor-semitrailer vehicles to achieve lane following. differential braking forces of the semitrailer are utilized to stabilize the trailer yaw motion and thus to prevent the potential occurrences of undesirable yaw instabilities such as trailer swing and jackknifing. In the design, they assumed perfect nonlinear model of the vehicle system. Tai and Tomizuka (1999) designed a Sliding Mode Controller (SMC) explicitly taking the model uncertainties into account. In SMC, the larger the moel uncertainty, the higher the control gain. In the heavy vehicle model, there exist both parametric uncertainty and unmodeled dynamics. To reduce the feedback gain for riding comfort purposes while maintaining the robust stability feature of the SMC technique, Tai and Tomizuka (1999) incorporated adaptivity of the noncertain parameters into the SMC. In doing so, different model uncertainties, parametric uncertainties and unmodeled nonlinear dynamics, are taken care of by different parts of the control scheme, namely, parameter adaptation and robust control.

There also have been several linear robust controllers proposed for the lateral control of heavy vehicles: Lead-lag controller (Wang and Tomizuka, 1998), H_∞ loop-shaping controller (Wang and Tomizuka, 1999), Linear Parameter Varying(LPV) controller (Hingwe and Tomizuka, 2000). One common point among above mentioned linear controllers is that the model used in controller design is abtained by linearizing the a nonlinear model about its operating point. Different linear robust control schemes are proposed by assuming different uncertainties models such as uncertainties in the coefficient matrices or uncertainties in the system parameters or acknowledging the time varying nature of some parameters.

Other than direct linearization, feedback linearization method can also convert a nonlinear system to a linear system. When the nonlinear system dynamics are exactly known and the relative degree is definite, then there exits a nonlinear state transformation and input redefinition which transforms the original nonlinear system to a linear system in the new coordinate system (Isidori,1992). This enables us to take advantage of linear controller design method without sacrificing in the accurate representation of system model dynamics. One restriction of the feedback linearization method is the assumption on the perfect knowledge of the original nonlinear system which is very hard to be satisfied. Nonetheless, the uncertain tractor-semitrailer model in the road coordinate system assumes a particular structure, a canonical form, and this structure enables the nonlinear uncertain model be transformed to a linear uncertain model. It is noted that the standard SMC implicitly uses feedback linearization.

In this chapter, we explore the use of feedback linearization in the design of two closely related but different nonlinear robust controllers for lateral guidance of tractor-semitrailer vehicles. One design resembles the ultimate bounded control approach originally proposed by Corless and Leitmann (1981). The other is based on sliding mode control. The basic philosophy behind the use of nonlinear robust control is to build robustness into the control algorithm. While this is a good idea, but whether it is the best approach from the practical point of view is not clear. The controllers rendered above are designed to robustly maintain small lateral errors. The other control objective, passenger comfort, is not directly addressed in controller design, and it must be checked and fine tuned by simulations and experiments. Thus, in the second part of this chapter, we will examine the two nonlinear robust controllers from the viewpoint of implementation. We will also review representative robust linear control algorithms.

3.2 System Model Description

The simplified control model of tractor-semitrailer heavy vehicles has 3 degrees of freedom: tractor lateral motion, tractor yaw motion and yaw motion of the semitrailer relative to the tractor. The road-vehicle interaction is represented by a linear function of tire slip angles. The simplified model used in the controller design throughout this chapter is derived using the method proposed in Tai and Tomizuka (1998) by setting the number of units equal to 2.

By utilizing the two sensor scheme in the magnetic reference sensing system, we can synthesize lateral error at any virtual look-ahead distance d_s (Patwardhan et al. 1997). Let the lateral error at the virtual sensor location in the road coordinate system be y_s, then the tractor-semitrailer dynamics in the road coordinate system is given as follows (Tai and Tomizuka, 1999).

$$\ddot{y}_s = b_x(q, \dot{q})\delta + f_x(q, \dot{q}) + \tilde{f}_x(q, \dot{q}, \dot{\epsilon}_d) \tag{3.1}$$

where, $q = [\int V_y, \epsilon_1, \epsilon_f]^T$, V_y is the lateral velocity of the center of gravity (c.g.) of the tractor, ϵ_1 is the tractor yaw angle, ϵ_f is the articulation angle, δ is the front wheel steering angle and $\dot{\epsilon}_d$ is the desired yaw rate imposed by the geometry of the road.

In (3.1), $f_x(q, \dot{q})$ is a nonlinear term, $\tilde{f}_x(q, \dot{q}, \dot{\epsilon})$ represents all terms that can not be modeled exactly (e.g. the nonlinear components of tire model and external disturbances). Considering the physical properties of the system, the following reasonable assumptions are made.

Assumption 3 *The unknown nonlinear function $\tilde{f}_x(q, \dot{q}, \dot{\epsilon}_d)$ is bounded above by a known function, $\alpha(q, \dot{q}, \dot{\epsilon}_d, t)$, i.e. $|\tilde{f}_x(q, \dot{q}, \dot{\epsilon}_d)| \leq \alpha(q, \dot{q}, \dot{\epsilon}_d, t)$.*

Assumption 4 *$b_x(q, \dot{q})$ is a positive function.*

Note that the first assumption is about the extent of model uncertainties. The second assumption is to ensure that the input gain in Eq.(3.1) is nonzero all the time.

3.3 Robust Feedback Linearization Controller Design

The traditional feedback linearization method assumes that we know the system exactly. The tractor-semitrailer system of Eq.(3.1) is nonlinear and has uncertainties. However, the system model satisfies matching conditions, i.e., the control action and the uncertainty are in the same channel. Therefore if we let

$$\delta = \frac{1}{b_x(q,\dot{q})}(-f_x(q, \dot{q}) + v) \tag{3.2}$$

then, the system dynamic equation becomes

$$\ddot{y}_s = v + \tilde{f}_x(q, \dot{q}, \dot{\epsilon}) \tag{3.3}$$

The resulting system is a second order linear system with model uncertainty. By further letting $x = [y_s, \dot{y}_s]^T$, we have

$$\dot{x} = Ax + Bv + B\tilde{f}_x(q, \dot{q}, \dot{\epsilon}) \tag{3.4}$$

where,

$$A = \begin{bmatrix} 0 & 1 \\ 0 & 0 \end{bmatrix}, \qquad B = \begin{bmatrix} 0 \\ 1 \end{bmatrix} \tag{3.5}$$

Note that the pair $[A, B]$ is controllable. If there is no uncertainty, i.e. $\tilde{f}_x(q, \dot{q}, \dot{\epsilon}) = 0$, then there exits a stabilizing state feedback controller, $v = -Kx$, where, K is chosen such that $A - BK$

has eigenvalues with negative real parts. To deal with the uncertainty, we use the robust control law

$$v = -Kx - W \tag{3.6}$$

where W is a scalar to be designed. Then

$$\dot{x} = (A - BK)x + B\tilde{f}_x(q, \dot{q}) - BW \tag{3.7}$$

Let a candidate Lyapunov function be given by $V(x) = x^T P x$, where $P \in \mathbf{R^{2\times 2}}$, $P \succ 0$, $P^T = P$ and P satisfies

$$(A - BK)^T P + P(A - BK) + Q \preceq 0 \tag{3.8}$$

for some $Q \succeq 0$. Then, the time derivative of $V(x)$ along the system dynamics (3.7) is

$$\begin{array}{rcl} \dot{V} & = & \dot{x}^T P x + x^T P \dot{x} \\ & = & x^T[(A - BK)^T P + P(A - BK)]x \\ & & -2x^T PB(W - \tilde{f}_x(q, \dot{q})) \\ & \leq & -x^T Q x - 2x^T PB(W - \tilde{f}_x(q, \dot{q})) \end{array} \tag{3.9}$$

Let

$$W = \alpha(q, \dot{q}, t) sgn(x^T PB) \tag{3.10}$$

then

$$-2x^T PB(W - \tilde{f}_x(q, \dot{q})) \leq 0 \tag{3.11}$$

¿From (3.9) and (3.11), we have

$$\dot{V} \leq -x^T Q x \leq 0 \tag{3.12}$$

By combining (3.2), (3.6) and (3.10), the control input is given by

$$\delta = \frac{1}{b_x(q,\dot{q})}(-f_x(q, \dot{q}) - Kx - \alpha(q, \dot{q}, t) sgn(x^T PB)) \tag{3.13}$$

Theorem 2 *(3.13) is an asymptotically stabilizing control law for system (3.1).*

3.4 Comparison of Robust Linear Feedback Controller with SMC

Eq.(3.13) is a robust discontinuous controller with a close resemblance to the sliding mode controller. Tai and Tomizuka(1999) designed a sliding mode controller for the tractor-semitrailer system in the context of AHS. It is given by

$$\begin{array}{rcl} \delta & = & \frac{1}{b_x(q,\dot{q})}(-f_x(q, \dot{q}) + \ddot{y}_d - \lambda \dot{e} - (\alpha + k) sgn(S)) \\ e & = & y_s - y_d \\ S & = & \dot{e} + \lambda e \end{array} \tag{3.14}$$

where, y_d is the desired trajectory, λ and k are positive positive control parameters. If we let the desired trajectory be 0, then

$$\begin{array}{rcl} \delta & = & \frac{1}{b_x(q,\dot{q})}(-f_x(q, \dot{q}) - \lambda \dot{y}_s \\ & & -(\alpha(q, \dot{q}, t) + k) sgn(\dot{y}_s + \lambda y_s)) \end{array} \tag{3.15}$$

On the other hand, the controller (3.13) can be rewritten as

$$\begin{aligned}\delta &= \tfrac{1}{b_x(q,\dot{q})}(-f_x(q,\dot{q}) - k_2\dot{y}_s - k_1 y_s \\ &\quad -\alpha(q,\dot{q},t)sgn(p_{22}\dot{y}_s + p_{12}y_s)) \\ &= \tfrac{1}{b_x(q,\dot{q})}(-f_x(q,\dot{q}) - k_2\dot{y}_s - k_1 y_s \\ &\quad -p_{22}\alpha(q,\dot{q},t)sgn(\dot{y}_s + \tfrac{p_{12}}{p_{22}}y_s))\end{aligned} \tag{3.16}$$

where we expanded the matrices K and P in their components. In terms of the matrix components, the condition that P is symmetric positive definite is equivalent to

$$\begin{aligned}&p_{11} > 0 \\ &p_{22} > 0 \\ &p_{12} = p_{21} \\ &p_{11}p_{22} - p_{12}p_{21} > 0\end{aligned} \tag{3.17}$$

Comparing Eq.(3.15) and Eq.(3.16), we see that $\frac{p_{12}}{p_{22}}$ corresponds to λ which defines a "sliding surface" in the sliding mode control. In the sliding mode control, λ is chosen in such a way that it defines a stable manifold, i.e, $\lambda > 0$. Interestingly, in the feedback linearization design, p_{12} could be a negative number. This is because of the different stabilizing principles in the two controller design schemes. In SMC control, the robust control law for δ given by Eq.(3.15) only guarantees that the first order dynamics of the sliding surface, S, is robustly stable and on the manifold defined by S, the choice of the λ ensures the stability within the manifold. It is a two step stabilization strategy. However, in the robust feedback linearization control, the control law for δ given by Eq.(3.16) guarantees the stability of the second order system dynamics by itself.

In sliding mode control, the coefficient of the discontinuous term is $\alpha(q,\dot{q},t) + k$, whereas in the proposed control, the coefficient of the discontinuous term is $p_{22}\alpha(q,\dot{q},t)$. Note that the inequality (3.8) still holds when mulitplied by a scalar. Therefore, without loss of generality, we can always assume that $p_{22} = 1$. In sliding mode cotrol, the additional positive parameter k is added in the coefficient of the discontinuous term to ensure the finite time convergence of the states to the manifold of the sliding surface, and therefore it is not desirable to select k too small. Once the sliding surface is reached in finite time, the system states go to the equilibrium asymptotically while staying on the manifold. In the feedback linearization, all the states goes to the equilibrium point asymptotically in the state space. It is not difficult to see that the sliding mode controller will inevitably results in a higher gain controller and degrades riding comfort. The situation remains the same when saturation functions replace the sign functions to reduce chattering in both feedback linearization controller and sliding mode controller.

For fairness of comparison, the SMC is modified as follows.

$$\begin{aligned}\delta &= \tfrac{1}{b_x(q,\dot{q})}(-f_x(q,\dot{q}) - \lambda\dot{y}_s - k(\dot{y}_s + \lambda y_s) \\ &\quad -(\alpha(q,\dot{q},t))sgn(\dot{y}_s + \lambda y_s))\end{aligned} \tag{3.18}$$

Comparing the modified sliding mode controller (3.18) and feedback the linearization controller (3.16) and assuming that there is no model uncertainty, i.e. $\alpha(q,\dot{q},t) = 0$, we note that both Eq.(3.16) and Eq.(3.18) stabilize the linear system (3.4). In the case of modified sliding mode control, the characteristic equation of the closed loop system is

$$s^2 + (\lambda + k)s + \lambda k = 0 \tag{3.19}$$

and, in the case of feedback linearization based control, the closed loop characteristic equation is

$$s^2 + k_2 s + k_1 = 0 \tag{3.20}$$

As we can see, in the modified sliding mode control, the dynamics of the sliding surface/manifoldand and that of the nominal system is coupled whereas, in the robust feedback linearization control, the dynamics of the "sliding surface" and that of the nominal plant are decoupled. If we can find a positive definite matrix P satisfying Linear Matrix Inequality (3.8) with $p_{22} < 1$, we are equivalently "minimizing" the magnitude of the model uncertainty. It is obvious that we always can find such a P, by simultaneously scaling P and Q in (3.8).

Both in the robust feedback linearization control and SMC, we assume that the zero dynamics of the system is stable and the designed controllers robustly stabilize the r dimensional controllable subspace, where, r is the relative degree of the dynamic system. In the SMC, the r dimensional controllable subspace is described as a set of $r-1$ dimensional stable submanifolds, i.e. 1 dimensional submanifold space, and the stability is achieved in two stages: First the 1 dimensional submanifold space is force to converge to zero by the sliding mode controller and then, from the stability of the submanifolds, the system state converges to zero. In the robust feedback linearization controller, the controller forces the state in the r dimensional controllable subspace goes to zero. Hence, there is no stability requirement for the submanifold, $x^T PB = 0$.

Another thing that we would like to point out is that, we can optimaly select the control parameters in the robust feedback linearization control method.

3.5 Simulation Results

In the design of robust controllers, we assumed that the model uncertainty is bounded by a know function (Assumption 3). In practice it is very hard to evaluate the uncertainty bound. In simulations, the tire cornering stiffness is perturbed 50% to introduce more uncertainties in addition to the unmodeled nonlinear dynamics. We assume that the uncertainty bound is time and state invariant, i.e. $\alpha(q, \dot{q}, t) = \alpha$. To estimate the uncertainty bound, the control parameter k was set to zero in the sliding mode controller (3.15), and repeatedly run simulations by increasing α by a small amount ($\Delta\alpha$) each time. We expect that when α changes from some value smaller than the true bound, say α^* to some value larger than the true value, the system will change from an unstable system to a stable one. Since, α is increased by a finite amount in each simulation, the uncertainty bound is set to the value at which stability is attained for the first time. This procedure should be repeated for each selected simulation scenaros.

The simulation scenario for a tractor-semitrailer at a velocity of $60mph$ is as follows. Initially the vehicle travels on a straight section for 0.5 second; at $t = 0.5sec$, it enters a curved section with a radius of $600m$; and at $t = 3sec$, it leaves the curved section and continue to run on a straight section. By the method mentioned above, we conclude that the uncertainty bound α is 0.30. In Fig. (3.1), the dotted lines are the simulation results of the SMC with $k = 0.01$ and $\alpha = 0.30,\ 0.33,\ 0.35,\ 0.37$ respectively from top to the bottom and the solid lines are the simulation results of the robust feedback linearization controller with $K = [2,\ 1]^T$, $Q = [1\ 0;\ 0\ 1]$ and $\alpha = 0.30,\ 0.33,\ 0.35,\ 0.37$ respectively from top to the bottom. The left top plot is the designed control input, the left bottom plot is the lateral error at the center of gravity of the tractor, the right top plot is the relative yaw error of the tractor and the right bottom plot is the lateral acceleration of the tractor.

From the plot of the lateral error and the relative yaw error of the tractor, we see that SMC is very sensitive to the knowledge of the uncertainty bound, and once the bound is known, any

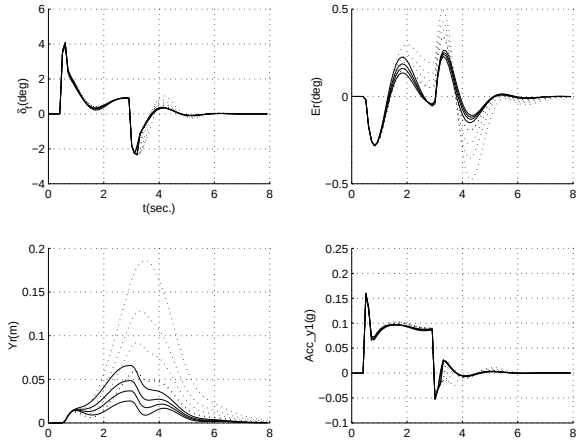

Figure 3.1: Simulation results

positive number k will stabilize the system. In the robust feedback linearization control (RFLC), due to the $-x^T Qx$ term in the $\dot{V}$, even smaller estimation of the uncertainty bound can stabilize the system. SMC is a robust stabilizing controller and it is very hard to incorporate performance criteria in controller design, while in the case of RFLC, it is easy to incorporates performance criteria in the controller design with the different selection of K and Q and there is possibility of optimally selecting the control parameters using the semidefinite programming method.

3.6 Implementation of Vehicle Lateral Controllers

As stated in Section 3.2, the vehicle dynamics is nonlinear. Thus, linear controllers are designed after linearizing the nonlinear dynamic equation around an operating point. As the vehicle's state further deviate from the operating point, the approximation error enlarges. This necessitates the need of gain scheduling. On the other hand, feedback linearization cancels the nonlinear term, and the remaining part of the control law, including linear feedback terms if any, may be fixed over the entire operating range. As stated in introduction, two major control objectives in the vehicle lateral control problem are to maintain small lateral errors and to ensure passenger comfort. While there are not many passengers on tractor-semitrailer vehicles, the lateral accelerations and jerks must remain at reasonable levels. In robust nonlinear control algorithms, there is no explicit method to ensure that the controller may ensure passenger comfort. The smoothness of the steering input is one of the most important aspect from the viewpoint of public acceptance of automated driving. It affects not only the lateral jerk and acceleration, i.e. passenger comfort, but most passengers do not like the oscillatory steering action. Thus, the final tuning of controllers must be performed by experiments.

Table 1 summarizes some important aspects in the implementation of control algorithms. For comparison, the table includes two other representative robust controllers developed for lateral guidance. They are the H_∞ loop shaping controller (Wang and Tomizuka,1999) and the LPV controller (Hingwe, Packard and Tomizuka, 2000). The performance of each controller strongly depends on the design parameters in the table. Selection of these parameters requires good

understanding of vehicle dynamics, control objectives and limitations of actuators. In terms of input variables, every control algorithm depends on the lateral errors measured at the front and rear ends of the trailer. Linear controllers utilize only the lateral sensors. It turns out that the lateral error measurements by magnetometers are least contaminated by measurement noise, which is a reason that the implementation of linear control algorithms has been relatively easy compared to that of nonlinear control algorithms. Nonlinear robust control algorithms require many other variables primarily for the computation of the feedback linearization term.

The fixed gain linear robust controller is easiest to implement. To provide a uniform and consistent stability robustness and performance, gain scheduling is required. The H_∞ robust controller with gain scheduling has been successfully implemented although its performance is yet to be optimized. The LPV controller is computer intensive both in design and implementation. It has, however, been designed on the top of experience gained by the implementation of linear controllers including the H_∞ robust controller, and it has also been successfully implemented. In fact, the LPV controller provides the smoothest steering action. As stated in Table 1, it has been implemented as a 16 states, linear interpolation-gain scheduling controller. While the feedback linearization is a sound analytical idea, the computation of the necessary term requires many variables as listed in the table. Among them, the lateral velocity is not directly measurable and must be estimated. It turns out that this is not a trivial problem to solve because the lateral error measurements based on magnets are intermittent. Error measurements may be fused with the output of the lateral accelerometer, but it is biased and is contaminated by noise. The nonlinear robust controller based on sliding mode has been tested only at low speeds less than 20 miles/hours, where the exact cancellation of the nonlinear term is not critical.

Experimental work has been performed at Crows Landing, an abandoned airfield near the US Interstate 5 about 90 miles away from Berkeley. The location of the test site makes it difficult to continue testing on daily basis. Nevertheless, both the H_∞ loop shaping controller and the LPV controller have been successfully tested at speeds reaching $55mph$ on the test track at the Crows Landing, which is about $2km$ long and has series of curveswith $800m$ radius. Experimental results are in Hingwe, et al (1999) and Hingwe, Packard and Tomizuka (2000).

3.7 Conclusions

In this chapter, we introduced some additional aspects to the design of nonlinear robust controllers for lateral control of tractor-semitrailer heavy vehicles. The new approach is to directly synthesize the robustness term based on a quadratic Lyapunov function. It resembled the ultimate bounded control approach. The second part of the chapter considered practical issues related to the implementation of various lateral control algorithms. To date, we have successfully implemented linear robust controllers, and the implementation of nonlinear robust controllers requires some further effort.

Chapter 4

Robust H_∞ Controller

This chapter deals with the robust steering control problem for heavy-duty vehicles (HDVs) in automated highway system (AHS) using a H_∞ loop shaping design procedure. In particular, a robust H_∞ steering controller utilizing the virtual-look-ahead methodology is designed for a tractor-semitrailer to track the road centerline on both curved and straight highway sections. It is robust to the model uncertainties which consist of vehicle longitudinal speed, road adhesion coefficient and cargo loads in the trailer. Numerical simulations and experiments on a test truck show the effectiveness of the proposed controller.

Keywords: *H_∞ loop shaping, robust lateral control, Heavy-Duty Vehicles.*

4.1 Introduction

Automated Highway System (AHS) technologies have attracted growing attention among researchers throughout the world in the past several years. AHS technologies offer a number of benefits including the saving of fuel costs and the reduction of driver's stress. The ratio of automation cost and vehicle cost is much lower for Heavy-Duty Vehicles (HDVs) than for passenger vehicles. These aspects make AHS technologies particularly attractive for HDVs. The California PATH (Partners for Advanced Transit and Highways) Program has conducted an AHS study focused on HDVs since 1993. Chen and Tomizuka [29] developed a control model of single-unit HDV (tractor-semitrailer type) for AHS and designed a nonlinear steering and braking controller using the input-output linearization in [1]. Modeling of multi-unit HDVs was conducted by Tai and Tomizuka in [30] recently. This chapter addresses the robust steering control problem for a single HDV (tractor-semitrailer type) using H_∞ loop shaping design procedure (LSDP) which was proposed by McFarlane and Glover [31]. It was pointed out that variations of vehicle longitudinal speed and road adhesion coefficient have significant influence on vehicle dynamics (Patwardhan et al [44] for passenger cars ; Wang and Tomizuka [32] for HDVs). Varying cargo loads is another important cause of uncertainties for HDVs. Robustness against these model uncertainties will be discussed in the H_∞ synthesis. General speaking, H_∞ loop shaping is essentially a two stage design procedure. First, the open-loop plant is augmented by pre and post-weighting filters to give a desired shape for the singular values of the open-loop frequency response. The resulting shaped plant is then robustly stabilized with respect to coprime factor uncertainty using H_∞ optimization. Controllers obtained by H_∞ loop shaping have some advantages over other H_∞-based methods. For instance, no γ-iteration is needed for the solution, and explicit formula for the corresponding controllers are available. In particular, they do not

exhibit the stable pole-zero cancellation, which is common in many H_∞ control problems and is undesirable if the plant has lightly damped modes (Sefton and Glover [34] , Tsai et al [35]). This method has been successfully applied to several industrial problems (Hyde [36], Postlethwaite and Walker [37], and Fujita et al [38]). Mammar [39] and O'Brien et al [40] conducted similar approaches on automated passenger vehicles.

The remainder of the chapter is organized as follows. In Section 4.2, a linearized vehicle control model for HDV is presented, then control objectives and constraints are specified. Essential theoretical background for H_∞ loop shaping design is reviewed in Section 4.3. Controller synthesis and numerical simulations are shown in Section 4.4. Section 4.5 presents the experimental results showing the effectiveness of the proposed controller. Finally, conclusions are given in Section 4.6.

4.2 HDV Modeling and Control Objectives

4.2.1 Linearized HDV Model

Lateral control of vehicles for AHS consists of lane following and lane changing maneuvers. This report is concerned with lane following. The HDV model used in the chapter is from [29]. It is essentially a nonlinear model based on assumptions that the roll motion is negligible, that the longitudinal acceleration is small and that the tire force can be modeled linearly. With further assumptions of small yaw angle of the tractor relative to the road (ϵ_r) and small articulation angle between the tractor and semitrailer (ϵ_f), the linearized HDV model is:

$$M\ddot{q} + D\dot{q} + Kq = F\delta + E_1\dot{\epsilon}_d + E_2\ddot{\epsilon}_d \tag{4.1}$$

where

$$q = [\ y_r \quad \epsilon_r \quad \epsilon_f\ ]^T \tag{4.2}$$

is the generalized coordinate vector, y_r is the lateral displacement of the tractor's center of gravity (cg), δ (steering angle) is the control input and $\dot{\epsilon}_d$ and $\ddot{\epsilon}_d$ are the yaw rate and yaw acceleration of the road frame respectively. $\dot{\epsilon}_d$ can be represented by $v\rho$ (v is the vehicle longitudinal speed and ρ is the road curvature) and $\ddot{\epsilon}_d$ can be represented by $v\dot{\rho}$ (assume constant v), which are treated as disturbances to the system. Detail descriptions of the inertial matrix M, the damping matrix D, the stiffness matrix K, coefficient matrices F, E_1 and E_2 are given in [32]. Note that M is a function of m_2 (cargo loads in the trailer) and D is a function of v, m_2 and μ (road adhesion coefficient, 1 for dry road surface and 0.5 for wet road surface). F and K are functions of μ. Variation of these parameters will cause model uncertainties which will be discussed later in section 4.4. By defining the 6×1 state vector

$$x = \begin{bmatrix} q \\ \dot{q} \end{bmatrix} \tag{4.3}$$

the linear state-space model is obtained as

$$\begin{aligned} \frac{d}{dt}x &= \begin{bmatrix} 0 & I \\ -M^{-1}K & -M^{-1}D \end{bmatrix} x + \begin{bmatrix} 0 \\ M^{-1}F \end{bmatrix} \delta \\ &\quad + \begin{bmatrix} 0 \\ M^{-1}E_1 \end{bmatrix} \dot{\epsilon}_d + \begin{bmatrix} 0 \\ M^{-1}E_2 \end{bmatrix} \ddot{\epsilon}_d \end{aligned} \tag{4.4}$$

4.2.2 Virtual Look Ahead

Define y_s as the lateral displacement of the virtual look-ahead sensor which is placed d_s meters ahead of the tractor cg, i.e.

$$y_s = y_r + d_s \epsilon_r \tag{4.5}$$

The lateral error at the virtual sensor is obtained from the extrapolation of two magnetometer readings (they are located at the front axle and the rear axle of the tractor respectively). As shown in [44] and [32], by regulating y_s instead of y_r to zero, we can increase the phase lead of the system dynamics and have more damped zeros for the open-loop system. Increasing d_s provides larger phase lead even at high speeds. However there may exist a large lateral offset error at the tractor cg and the sensor noise will be amplified if a large look-ahead distance d_s is chosen. Thus there is a trade-off between the maximum phase margin we can get by redefining the output and the tracking performance we can achieve by regulating y_s. In this chapter, we choose $d_s = 5$ m for the controller design and implementation.

4.2.3 Control Objectives and Constraints

Considering the average lane width on US highways and the average width of the HDVs, a small lateral tracking error at the tractor cg is required (less than 0.2 m). Since the trailer is relatively long, small off-tracking error at the rear of the trailer is also desired. The designed controller should be robust against model uncertainties. We assume that the speed range for HDV is $0 \sim 25$ m/s ($0 \sim 56.25$ mph) and that the road adhesion coefficient varies from $\mu = 0.5$ to $\mu = 1$. Cargo loads in the trailer varies from $m_2 = 5000$ kg to $m_2 = 24000$ kg. The steering action is generated by the steering actuator which has a limited bandwidth. The steering rate is limited to 28 degree/s and steering angle is confined to 30 degree. In simulation, an additional time delay of 15 ms is added to the approximated first-order steering actuator dynamics.

4.3 H_∞ Loop Shaping Design - Theoretical Backgrounds

4.3.1 Robust Stabilization Problem

We will consider the stabilization of a plant G which has a normalized left coprime factorization (NLCF) (N, M):

$$G = M^{-1}N \tag{4.6}$$

A perturbed plant G_Δ can be written as

$$G_\Delta = (M + \Delta_M)^{-1}(N + \Delta_N) \tag{4.7}$$

where Δ_M and Δ_N are stable unknown transfer functions which represent the uncertainty in the nominal plant model G. The objectives of robust stabilization is to stabilize not only the nominal plant G but also a family of perturbed systems defined by

$$G_\Delta \quad = \quad \{(M + \Delta_M)^{-1}(N + \Delta_N) : \Delta = [\Delta_M \Delta_N] \in D_{S\epsilon}\} \tag{4.8}$$

where

$$D_{S\epsilon} = \{\Delta : \Delta \in RH_\infty, \|\Delta\|_\infty < \epsilon\} \tag{4.9}$$

The following theorem gives the necessary and sufficient conditions for the stabilizing controller K.

Theorem: The controller K stabilizes $G_\Delta = (M + \Delta_M)^{-1}(N + \Delta_N)$ in Fig.4.1 for all $\Delta = [\Delta_M \Delta_N] \in D_{S\epsilon}$ iff
(a) K stabilizes G.
(b)

$$\gamma = \| \begin{bmatrix} K \\ I \end{bmatrix} (I - GK)^{-1} M^{-1} \|_\infty \leq \epsilon^{-1} \tag{4.10}$$

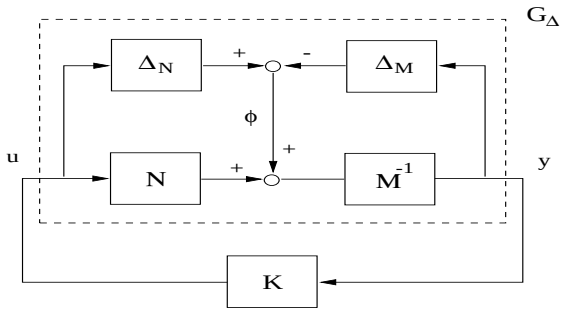

Figure 4.1: H_∞ robust stabilization problem

Note that γ is the H_∞ norm from ϕ to $[u\ y]^T$ and $(I - GK)^{-1}$ is the sensitivity function for this positive feedback arrangement shown in Fig.4.1. The lowest achievable value of γ and the corresponding maximum stability margin ϵ are given by [31]:

$$\begin{aligned} \gamma_{min} &= \epsilon_{max}^{-1} = \{1 - \|[NM]\|_H^2\}^{-1/2} \\ &= (1 + \rho(XY))^{-1/2} \end{aligned} \tag{4.11}$$

where $\|\cdot\|_H$ denotes the Hankel norm and ρ denotes the spectral radius (the maximum eigenvalue). X and Y are the unique positive definite solutions of the following algebraic Ricatti equations:

$$\begin{aligned} (A - BS^{-1}D^TC)^TX + X(A - BS^{-1}D^TC) \\ -XBS^{-1}B^TX + C^TR^{-1}C = 0 \end{aligned} \tag{4.12}$$

and

$$\begin{aligned} (A - BS^{-1}D^TC)Y + Y(A - BS^{-1}D^TC)^T \\ -YC^TR^{-1}CY + BS^{-1}B^T = 0 \end{aligned} \tag{4.13}$$

where

$$R = I + DD^T, S = I + D^TD \tag{4.14}$$

A "central" controller proposed in [31], which guarantees that

$$\| \begin{bmatrix} K \\ I \end{bmatrix} (I - GK)^{-1}M^{-1} \|_\infty \leq \gamma \tag{4.15}$$

for a specified $\gamma > \gamma_{min}$, is given by

$$A_K = A + BF + \gamma^2(L^T)^{-1}YC^T(C + DF) \tag{4.16}$$

$$\begin{aligned} B_K &= \gamma^2(L^T)^{-1}YC^T \\ C_K &= B^TX \\ D_K &= -D^T \end{aligned}$$

$$F = -S^{-1}(D^TC + B^TX) \tag{4.17}$$

$$L = (1 - \gamma^2)I + XY \tag{4.18}$$

where (A_K, B_K, C_K, D_K) is the state-space realization of the central controller K. Since γ_{min} can be computed from Eq.(4.11), we can get an explicit solution by solving just two Ricatti equations (Eqs.(4.12) and (4.13)) thus avoiding the γ-iteration needed to solve the general H_∞ problem.

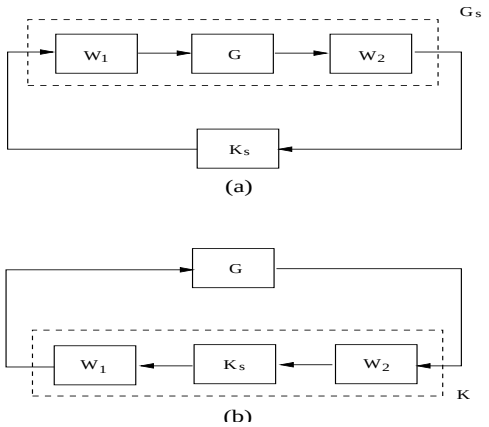

Figure 4.2: The Shaped Plant and Controller

4.3.2 H_∞ Loop Shaping Design Procedure (LSDP)

Robust stabilization alone is not practical because the designer is not able to specify any performance requirements. McFarlane and Glover [31] proposed pre- and post-compensation of the plant to shape the open-loop singular values prior to robust stabilization of the "shaped plant". First, choose W_1 and W_2 as the pre- and post-weighting filters respectively; the resulting shaped plant G_S is given by

$$G_S = W_2 G W_1 \tag{4.19}$$

as shown in Fig.4.2 (a). Next the controller K_S is synthesized by solving the robust stabilization problem (Section 4.3.1) for the shaped plant G_S with a NLCF: $G_S = M_S^{-1} N_S$. Finally the feedback controller for the plant G is realized as $K = W_1 K_S W_2$ (see Fig.4.2 (b)). Note that the maximum stability margin ϵ_{max} (Eq.(4.11)) indicates the magnitude of the maximum allowable perturbation of the shaped plant G_S. In this procedure, ϵ_{max} is treated as a design indicator of the proposed controller.

4.4 Controller Synthesis and Simulation

As mentioned in Section 4.2.2, we will utilize the advantages of virtual-look-ahead methodology in the controller design. From Eq.(4.4) and Eq.(4.5), we can get the transfer function from the steering angle (δ) to the lateral error at the virtual sensor (y_s) (define it as $G_P(s)$). The nominal operating condition is selected as $v = 18$ m/s, $\mu = 0.8$ and $m_2 = 10670$ kg. If we have a good inner-loop controller, the steering actuator can be modeled as a first-order dynamics approximately (represent it as $G_A(s)$). The nominal plant $G(s)$ is defined as $G(s) = G_P(s)G_A(s)$. To avoid the chattering of the steering column generated by high bandwidth steering actuator, the steering command is filtered with a low-pass filter $W_2(s)$:

$$W_2(s) = \frac{1}{5s+1} \tag{4.20}$$

A constant gain 2 is chosen for $W_1(s)$ to obtain the desired small tracking error. Since windup may deteriorate the system performance, we do not put an integral action in $W_1(s)$ and $W_2(s)$. On the other hand, the H_∞ synthesized controller will have at least the same order as the shaped plant, thus the orders of the weighting filters should be kept as small as possible. In this case,

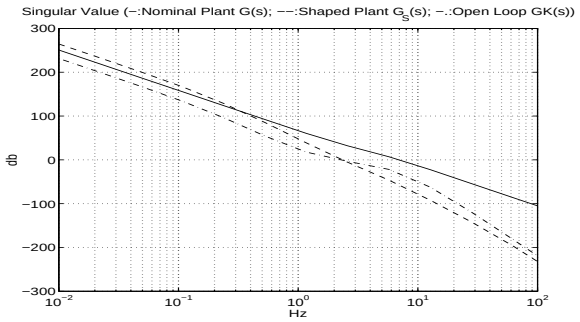

Figure 4.3: Singular values of the nominal plant $G(s)$ (–), the shaped plant $G_S(s)$ (- -) and the open-loop transfer function $GK(s)$ (-·)(with reduced-order controller)

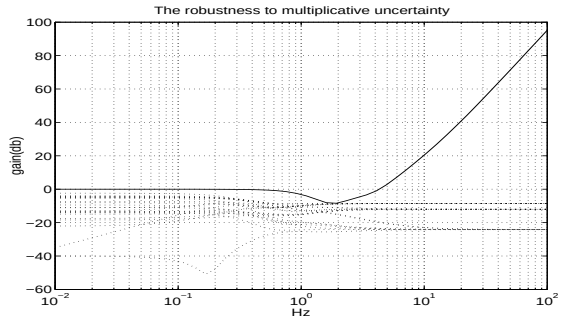

Figure 4.4: The maximum allowable multiplicative uncertainty (solid line) and multiplicative uncertainties caused by varying $v(0 \sim 25$ m/s), $\mu(0.5 \sim 1)$ and $m_2(5000$ kg ~ 24000 kg).

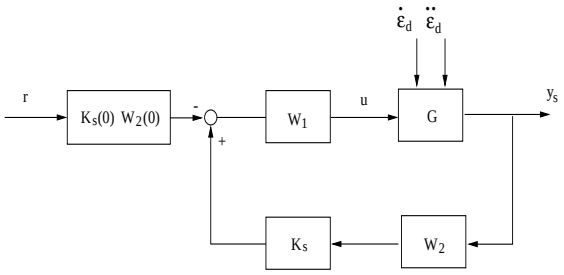

Figure 4.5: Implementation of the controller

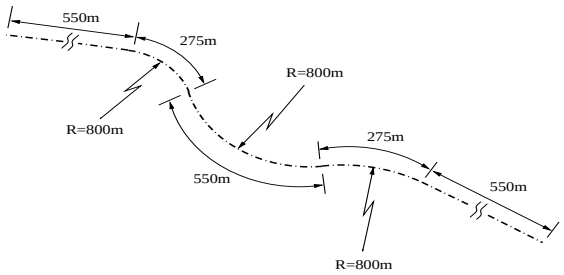

Figure 4.6: Scheme of the Crows Landing test cite

the shaped plant $G_S(s)$ is eighth order and its singular value is shown in Fig.4.3. Applying above LSDP, we obtain a H_∞ loop shaping controller $K_S(s)$ with $\epsilon_{max} = 0.2053$. After cascading the shaping filters, it turns out to be a ninth order. Using the balanced residualization method (Fernando and Nicholson [41]) to reduce the cascaded controller $K(s)$, the order is reduced to four. The singular values of open-loop transfer function $GK(s)$ (with reduced controller $K(s)$) is also shown in Fig.4.3. The maximum allowable multiplicative plant perturbation for closed-loop stability can be computed by $1/\bar{\sigma}(GK(I-GK)^{-1})$. As seen from Fig.4.4, the multiplicative uncertainties (dotted line) caused by varying $v(0 \sim 25$ m/s), $\mu(0.5 \sim 1)$ and $m_2(5000$ kg ~ 24000 kg) are smaller than the maximum allowable value (solid line).

The H_∞ loop shaping controller is implemented as shown in Fig.4.5. The road curvature is treated as a disturbance to the plant G by way of $\dot{\epsilon}_d$ and $\ddot{\epsilon}_d$. This configuration has some advantages over the conventional feedback control structure. For example, the reference does not directly excite the dynamics of $K_S(s)$, which may result in larger overshoot. The constant prefilter ensures a steady-state gain of 1 between reference input r (desired look-ahead trajectory) and y_s. Here r is set to be zero for regulation of y_s. The scenario for numerical simulation is selected to follow the test track at the Crows Landing test site (Fig.4.6). Figure 4.7 shows the simulation results for the nominal condition and two perturbed conditions. As seen from Fig.4.7, the steady-state lateral errors at the tractor front axle (y_{s1}), the tractor rear axle (y_{s2}) and the trailer rear axle (y_{s3}) are smaller than 0.1 m for the nominal condition and 0.2 m for perturbed conditions. However, the transient tracking errors can be as high as 0.45 m for perturbed conditions when entering curved sections at 825 m and 1375 m where the road curvature ρ is changing from $\mp 1/800$ m to $\pm 1/800$ m. Steering actions are smooth both on curved and straight sections which can ensure driver comfort and the extended life of the steering actuator/column.

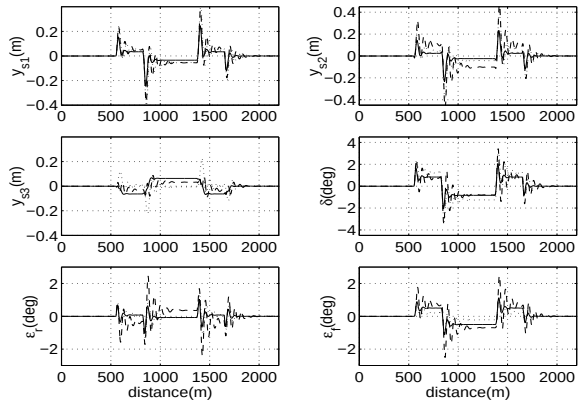

Figure 4.7: Closed-loop simulation: nominal condition (solid:$v = 18$ m/s, $\mu = 0.8$, $m_2 = 10670$ kg) and perturbed conditions (dashed:$v = 25$ m/s, $\mu = 1.0$, $m_2 = 24000$ kg) (dotted:$v = 20$ m/s, $\mu = 0.6$, $m_2 = 5000$ kg)

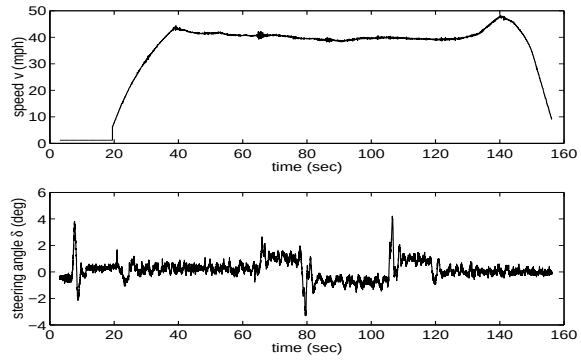

Figure 4.8: Vehicle longitudinal speed v (mph) (up) and steering angle δ (deg) (down)

4.5 Experiment Results

Some experimental evaluation of the proposed controller was performed on a Freightliner FLD 120 class-8 tractor with a semitrailer on the test track at Crows Landing. Although tests were performed only under limited conditions, the initial results were encouraging and correlated with simulation results well. Experimental results are shown in Fig.4.8 and Fig.4.9. Figure 4.8 shows the vehicle speed and the front wheel steering angle when the test vehicle was driven along the test track (Fig.4.6) under closed loop steering control. The speed was manually adjusted not to exceed 50 mph (upper plot in Fig.4.8). Large excursions of the steering angle when the vehicle arrives at points where the road curvature changes (lower plot in Fig.4.8) are consistent with the simulation results in the previous section (see Fig.4.7). Some noise signal is apparent in the plot of the steering angle, which is attributed to the vibration of the potentiometer placed close to the ground. In fact, the motion of the hand wheel was observed to be smooth. As shown in Fig.4.9, steady-state tracking errors of the tractor (y_{s1} and y_{s2}) are small on both straight road sections (< 0.15 m) and curved road sections (< 0.35 m). The off-tracking error is small at the rear axle of the trailer ($y_{s3} < 0.2$ m). This preliminary experiment validates the feasibility of

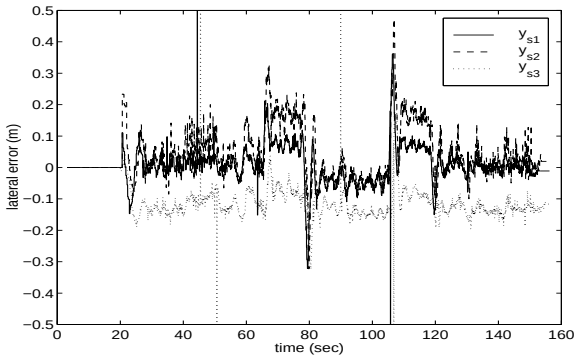

Figure 4.9: Lateral tracking error (m): lateral error at the tractor front axle (y_{s1}); lateral error at the tractor rear axle (y_{s2}); lateral error at the trailer rear axle (y_{s3})

the proposed controller which is robust under test speeds up to 45 mph.

4.6 Conclusion

In this chapter, a robust H_∞ loop shaping controller for the lateral control of HDVs in AHS was presented. By choosing the shaping factors (weighting filters) properly, good lane following with smooth steering action were achieved in the presence of plant uncertainties and external disturbances (curved road sections). Simulation results showed the robustness of the proposed controller. A preliminary experiment on the test truck at Crows Landing was conducted to validate the proposed controller.

Chapter 5

Gain-Scheduled H_∞ Loop-Shaping Controller

This chapter deals with the robust, gain-scheduled, lateral control problem for tractor-semitrailer combination vehicles (TSCVs) using an observer-structured H_∞ loop-shaping controller. Vehicle longitudinal speed is chosen as the scheduling parameter since variations of speeds dramatically change system dynamics in different frequency ranges. By utilizing the vehicle speed as the scheduling parameter, the controller minimizes the effect of uncertainties and nonlinearities, which depends mainly on the velocity. Two scheduling techniques are applied to evaluate the effectiveness of the proposed controller. Simulation shows that the gain-scheduled controller generally sustains a larger robstness region than the fixed-gain linear controller under the uncertainties of varying road adhesion coefficients and cargo loads in the trailer.

Keywords: *H_∞ loop-shaping, gain-scheduled control, tractor-semitrailer combination vehicles.*

5.1 Introduction

Automated guidance of heavy vehicles has been one of the active research topics on automated highway systems in recent years. Heavy vehicles have the potential of becoming the main beneficiaries of automated guidance for the following reasons. First, a truck travel six times the miles as compared to a passenger vehicle on average. Automation will reduce the operating cost substantially. Second, relative equipment-to-vehicle cost for automating heavy vehicles is far less than that for passenger vehicles. Third, automation of heavy vehicles will have a significant impact on the overall safety of highways. Trucking is a tedious job and automation will contribute substantially to reduce stress on the driver and, therefore, increase safety. Various uncertainties of the heavy vehicle system dynamics also make this research topic more interesting and challenging. For instance, varying vehicle longitudinal speed, tire cornering force and cargo loads dramatically change the system dynamics in different frequency ranges (see [32]). In favor of the controller design and simple dynamic analysis, dynamic models for single-unit heavy vehicles (tractor-semitrailer combinations) and multi-unit heavy vehicles are derived in [29] and [30] respectively. It has been confirmed by experiments that a linearized vehicle model can predict the dynamic frequency response of an actual tractor-semitrailer combination from the steering input to the lateral acceleration at speeds up to 20 m/s. At higher speeds, the model-

predicted response and the actual response significantly differ due to the nonlinearity of steering system and possible saturation of tire forces. In spite of such differences, carefully designed robust linear controllers have been shown to be effective (see for example, [42], [43], and [45]). Experimental validations of robust linear controllers are in [42] and [43]. The motivation of the work in this chapter is to incorporate as much knowledge about the main nonlinearities as possible into the control law. Variations of vehicle longitudinal speed cause noticeable system dynamic changes. For example, the higher the speed, the larger the phase lag around the gain cross-over frequency. Thus the vehicle speed is selected to be a gain-scheduling parameter. As an extension to the work done in [42], the designed H_∞ loop-shaping controller has an observer structure, which is suitable for gain-scheduling. Simulations have been performed to show that the gain-scheduled H_∞ loop-shaping controller has a larger robustness region than the fixed-gain controller. The remainder of the chapter is organized as follows. In section 5.2, a linearized vehicle control model for TSCVs is presented, and control objectives and constraints are specified. The observer-structured H_∞ loop-shaping controller is reviewed in section 5.3. Two interpolation methods are discussed in section 5.4. Simulation results for different gain-scheduled controllers are compared to the fixed-gain controller in section 5.5. Finally, section 5.6 gives the conclusions.

5.2 Lateral Control Problem for TSCV

5.2.1 Linearized Vehicle Model

Under the assumptions of negligible roll motion, constant longitudinal vehicle speed, and small yaw and articulation angles, the linearized vehicle dynamic equation can be written as:

$$\begin{aligned}\frac{d}{dt}x &= \begin{bmatrix} 0 & I \\ -M^{-1}K & -M^{-1}D(v) \end{bmatrix} x + \begin{bmatrix} 0 \\ M^{-1}F \end{bmatrix} \delta_f \\ &\quad + \begin{bmatrix} 0 \\ M^{-1}E(v) \end{bmatrix} \rho_d \\ &= A(v)x + B\delta_f + G(v)\rho_d \end{aligned} \tag{5.1}$$

where

$$\begin{aligned} x &= \begin{bmatrix} x_1 & x_2 & x_3 & x_4 & x_5 & x_6 \end{bmatrix}^T \\ &= \begin{bmatrix} y_r & \epsilon_r & \epsilon_f & \dot{y}_r & \dot{\epsilon}_r & \dot{\epsilon}_f \end{bmatrix}^T . \end{aligned}$$

y_r is the lateral error at the center of gravity of the tractor with respect to the road center line, ϵ_r is the relative yaw angle of the tractor with respect to the road center line, and ϵ_f is the articulation angle between the tractor and the trailer. δ_f is the front wheel steering angle. ρ_d is the curvature of road, which is treated as a disturbance to the plant. The contents of the inertia matrix M, the damping matrix D, the stiffness matrix K, and coefficient vectors F and E are shown in the Appendix. Note that M is a function of m_2 (cargo loads in the trailer), and D is a function of v (vehicle longitudinal speed) and μ (road adhesion coefficient). K and F are functions of μ assuming that the vehicle's physical parameters are fixed and E is function of v, μ and m_2. The controller input is the output of a real or virtual lateral error sensor located at d_s-meters ahead of the tractor's center of gravity: i.e,

$$y_s = y_r + d_s\epsilon_r \ . \tag{5.2}$$

Table 5.1: Estimated nominal parameters in the vehicle model

Symbols	Definitions (Nominal Value)
m_1	tractor mass (7727 kg)
m_2^*	semitrailer mass (10455 kg)
d_1, d_2	relative position (x,y) between tractor's C.G. to fifth wheel (3.26 m, 0.60 m)
d_3, d_4	relative position (x,y) between semitrailer's C.G. to fifth wheel (3.81 m, 1.20 m)
I_{z1}	tractor yaw moment of inertia (45926 kgm^2)
I_{z2}^*	semitrailer yaw moment of inertia (161780 kgm^2)
l_1	distance between tractor C.G. and front wheel axle (1.61 m)
l_2	distance between tractor C.G. and rear wheel axle (3.75 m)
l_3	distance between joint (fifth wheel) and semitrailer wheel axle (6.50 m)
μ^*	road adhesion coefficient (1.0) (0.5 for wet road; 1.0 for dry road)
$C_{\alpha f}^*$	cornering stiffness of tractor front wheel (180430.0 $\times$ μ N/rad)
$C_{\alpha r}^*$	cornering stiffness of tractor rear wheel (324774.0 $\times$ μ N/rad)
$C_{\alpha t}^*$	cornering stiffness of semitrailer rear wheel (324774.0 $\times$ μ N/rad)

When d_s is large, the "virtual" sensor is located ahead of the front bumper of the tractor, and y_s must be synthesized from the outputs of magnetometers at the front and rear bumpers ([44] and [32]). The lateral controller must be designed to decrease the phase lag around the cross-over frequency of the system dynamics and to provide phase lead even at high speeds.

5.2.2 Nominal Parameters

Estimated nominal parameters of the experimental vehicle (Freightliner FLD120 class 8 tractor and a Great Dane semitrailer) are shown in Table 5.1. Parameters with * mark in the table are considered to be uncertain and variations in these parameters are sources of uncertainties.

5.2.3 Control Objectives and Constraints

The lateral controller must be designed to ensure robust performance over the uncertainties caused by varying parameters such as m_2, μ and v. These parameters are considered varying in the following regions: $m_2 \in m_2^o \times [\ 0.5,\ \ 1.5\ ]\ kg$, $\mu \in [\ 0.5,\ \ 1.0\ ]$ and $v \in [\ 15,\ \ 35\ ]\ m/s$ where $(\bullet)^o s$ denotes the nominal values shown in Table 5.1. The lateral errors at the tractor front (y_{s1}) and rear(y_{s2}) ends and the lateral error at the trailer rear end (y_{s3}) are all required to be less than 0.2 m in consideration of the limited highway lane width. Smoothness of the steering action is desired to prevent the steering actuator/column from overheating or fatigue due to high frequency chattering. Since the vehicle dynamics depend on the speed in a significant way ([32]), the vehicle longitudinal speed is selected as the scheduling parameter in the design of gain-scheduled controllers to minimize the effect of nonlinearities and uncertainties, which depends mainly on the velocity.

5.3 Observer Structure of the H_∞ Loop-Shaping Controller

There have been few applications of gain-scheduled optimal controllers, because the linear controllers must all have the same structure such that the gains may be interpolated. Conventional PI controllers obviously have a clearly defined structure, and gain-scheduled multivariable PI controllers are also very straightforward. LQG controllers have been scheduled using the inherent plant observer structure of such controllers (see for example [46]). H_∞ controllers, in general, do not have such an explicit structure, and scheduling presents a problem. However, it was shown in [34] that the controller resulting from the loop-shaping approach can be written in an observer-structured form:

$$\dot{\hat{x}}_s = A_s\hat{x}_s + H_s(C_s\hat{x}_s - y_s) + B_s u_s \tag{5.3}$$

$$u_s = F_s\hat{x}_s \tag{5.4}$$

where $[A_s, B_s, C_s]$ is a state-space realization of the shaped plant (assumed to be strictly proper), $G_s(s) = W_2(s)G(s)W_1(s)$. $G(s)$ is the transfer function of the linearized plant (from δ_f to y_s). $W_1(s)$ and $W_2(s)$ are the pre- and post-shaping factors respectively. $H_s = -Y_s{C_s}^*$ and $F_s = -{B_s}^*(I - \gamma^{-2}I - \gamma^{-2}X_sY_s)^{-1}X_s$, where X_s and Y_s are solutions of the associated control and filtering algebraic Ricatti equations of the shaped plant:

$${A_s}^T X_s + X_s A_s - X_s B_s {B_s}^T X_s + {C_s}^T C_s = 0 \tag{5.5}$$

and

$$A_s Y_s + Y_s {A_s}^T - Y_s {C_s}^T C_s Y_s + B_s {B_s}^T = 0\ . \tag{5.6}$$

$\gamma > \gamma_{min} = \epsilon_{max}^{-1} = (1 + \rho(X_sY_s))^{1/2}$ where ϵ is the stability margin for the coprime factor uncertainty and ρ denotes the spectral radius. This clear structure lends itself to gain-scheduling in that the F_s and H_s gains can be scheduled as functions of vehicle longitudinal speed. Figure 5.1 shows a block diagram implementation of an observer-structured H_∞ loop-shaping controller where $P(v)$ is a pre-filter for the reference tracking problem. It does not have an effect on our specific regulation problem of automated guidance ($r = 0$). The structure has been verified to have good time-response properties, such as not exhibiting any overshoot, since the reference signal does not directly excite the controller dynamics.

5.4 Scheduling of Observer-structured H_∞ Loop-Shaping Controller

There are several scheduling techniques available for the proposed observer-structured H_∞ loop-shaping controller. The first method discussed in this chapter uses the simple linear interpolation. Assumptions on the smoothness of A_s, B_s and C_s with respect to the scheduling parameter are required. The second method is the so-called stability-preserving method [48], in which the interpolation method is obtained from solving the LMI (Linear Matrix Inequality) problems.

5.4.1 Linear Interpolation

In order to linearly interpolate between controller gains, the following conditions must be satisfied:
1. The shaped plant matrices A_s, B_s and C_s vary smoothly between operating points.
2. The controller gains F_s and H_s vary smoothly between operating points.

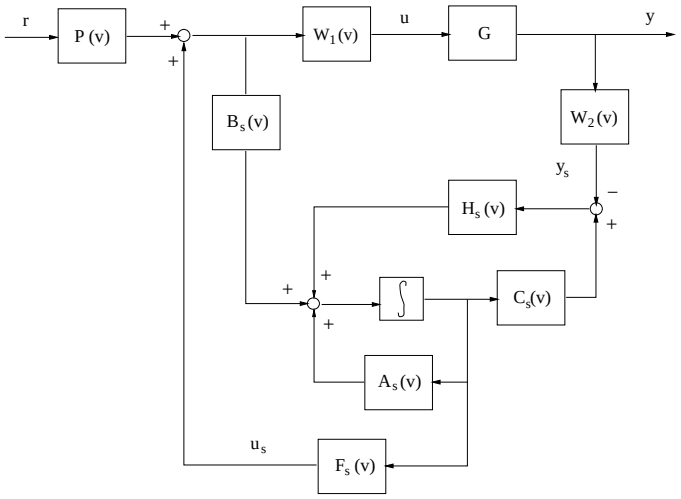

Figure 5.1: The implementation of the gain-scheduled H_∞ loop-shaping controller

From the analysis of the system dynamics in [32], if a sufficient number of operating points are chosen at different speeds such that the shaping factors vary smoothly from one point to another, the first condition can be satisfied. As indicated in [47], under the assumption of controllability and detectability of the shaped plant, the algebraic Ricatti solutions X_s and Y_s will be analytic functions of the scheduling parameter if the first condition is satisfied. This will ensure that the second condition is satisfied, and the interpolation of A_s, B_s, C_s, F_s and H_s is possible. For example, the F_s matrix between adjacent design points i and j would be calculated as

$$F_s(r) = (1-r)F_{si} + rF_{sj} \ , \ 0 \leq r \leq 1 \tag{5.7}$$

with $r = 0$ corresponding to the operating point i and $r = 1$ corresponding to the operating point j. The limitation of this approach is that a fixed structure is needed for the shaping factors so that they can be linearly interpolated.
For the automated guidance of TSCV, two linear controllers are designed at two different speeds, $v = 18$ and 30 m/s. As the vehicle travels, the controller parameters are linearly interpolated based on the vehicle longitudinal speed.

5.4.2 Stability-Preserving Interpolation

Another interpolation method uses the stability-preserving method. Basically, this interpolation method is addressed separately for the state feedback and state observer gains (for the theorems, refer to [48]). For the state feedback gains, F_{s18} (designed for $v = 18$ m/s) and F_{s30} (designed for $v = 30$ m/s), we compute symmetric positive-definite matrices N_{18} and N_{30} such that

$$N_i(A_s(v) + B_s(v)F_{si})^T + (A_s(v) + B_s(v)F_{si})N_i < -I$$
$$for \quad i = 18, 30 \tag{5.8}$$

where $v \in \left[\ 18, \quad 30 \ \right] \ m/s$. Theoretically N_i is needed to satisfy infinite LMIs. Alternatively we get the solution N_i at several points and check the solution is valid for a larger set of points.

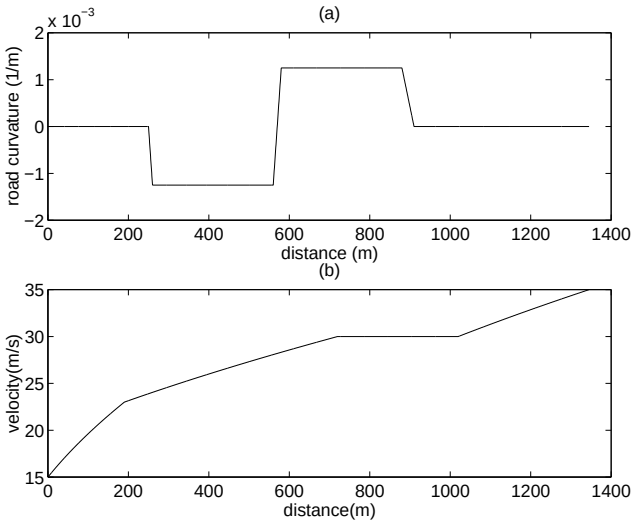

Figure 5.2: (a) The road curvature and (b) the vehicle speed

We choose a continuous state feedback gain

$$F_s(v) = \begin{cases} F_{s18} & v \leq 18 \\ \bar{F}_s(v)N^{-1}(v) & 18 < v < 30 \\ F_{s30} & v \geq 30 \end{cases} \tag{5.9}$$

where

$$\bar{F}_s(v) = \frac{30-v}{30-18}F_{s18}N_{18} + \frac{v-18}{30-18}F_{s30}N_{30} \tag{5.10}$$

$$N(v) = \frac{30-v}{30-18}N_{18} + \frac{v-18}{30-18}N_{30} \tag{5.11}$$

[48] shows that if $v(t)$ satisfies

$$|\dot{v}(t)| < \frac{|30-18|}{\|N_{30}-N_{18}\|} \qquad t \geq 0 \tag{5.12}$$

then the closed-loop time-varying linear system $\dot{x}(t) = (A_s(v(t)) + B_s(v(t))F_s(v(t)))x(t), \ \ t \geq 0$, is exponentially stable. Similarly, for the observer gains, H_{s18} and H_{s30}, suppose the symmetric positive definite matrices P_{18} and P_{30} are solutions to

$$P_i(A_s(v) + H_{si}C_s(v))^T + (A_s(v) + H_{si}C_s(v))P_i < -I \qquad for \quad i = 18, 30 \tag{5.13}$$

where $v \in \left[\ 18, \quad 30 \ \right] \ m/s$. We choose an observer gain

$$H_s(v) = \begin{cases} H_{s18} & v \leq 18 \\ P^{-1}(v)\bar{H}_s(v) & 18 < v < 30 \\ H_{s30} & v \geq 30 \end{cases} \tag{5.14}$$

where

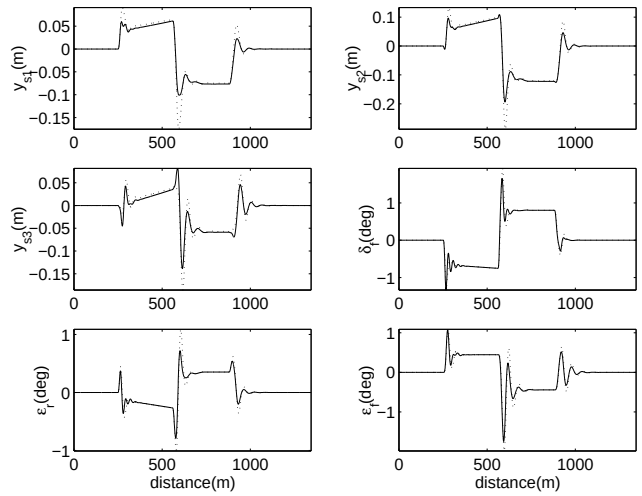

Figure 5.3: Closed-loop simulation for the nominal condition (dotted line: the fixed-gain controller)(solid line: the gain-scheduled controller using linear interpolation)

$$\bar{H}_s(v) = \frac{30-v}{30-18}H_{s18}P_{18} + \frac{v-18}{30-18}H_{s30}P_{30} \tag{5.15}$$

$$P(v) = \frac{30-v}{30-18}P_{18} + \frac{v-18}{30-18}P_{30} \tag{5.16}$$

If $v(t)$ satisfies

$$|\dot{v}(t)| < \frac{|30-18|}{\|P_{30}-P_{18}\|} \qquad t \geq 0\ , \tag{5.17}$$

the closed loop time-varying linear system $\dot{x}(t) = (A_s(v(t)) + H_s(v(t))C_s(v(t)))x(t), \quad t \geq 0$, is exponentially stable. We solve the LMI in Eqs. (5.8) and (5.13) such that $\|N_{30} - N_{18}\|$ and $\|P_{30} - P_{18}\|$ are minimized in order to get a larger allowable changing rate of the scheduling parameter.

5.5 Simulation Results

Two sets of controllers $(A_s, B_s, C_s, F_s, H_s)$ are respectively designed for two different speeds (operating points) at $v = 18$ and $30\ m/s$. For the lower speed, $18\ m/s$, $W_1(s) = 2$ and $W_2(s) = \frac{1}{2s+1}$ are chosen in the controller design. For the higher speed, $30\ m/s$, we set $W_1(s) = 2$ and $W_2(s) = \frac{1}{s+1}$, because the vehicle dynamics exhibit large phase lags around the cross-over frequency. First order actuator dynamics with a cross-over frequency near $2 \sim 3$ Hz are added to the vehicle transfer function from the steering input δ_f to the virtual lateral error y_s. The look-ahead distance is chosen to be $8\ m$. The road curvature profile used in simulation is shown in Figure 5.2(a). The truck enters a section with a constant road curvature of $-1/800\ m$ at $260\ m$ and leaves at $560\ m$. Then the truck enters another curved section with a road curvature of $1/800\ m$ at $580\ m$ and leaves at $880\ m$. The speed is assumed to be varying as shown in Figure 5.2(b) along the maneuver. Closed-loop simulations of the proposed

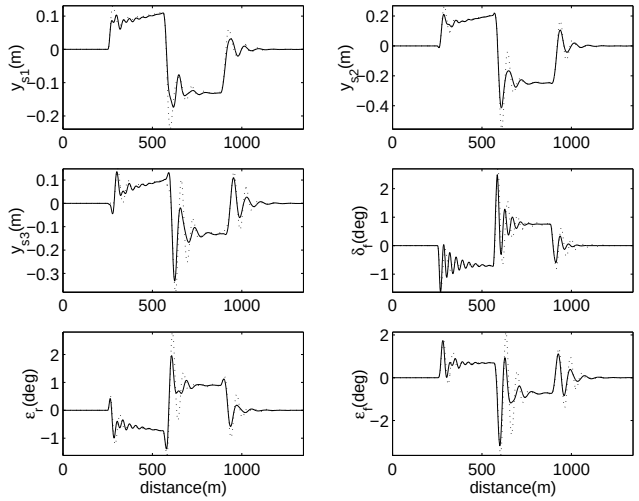

Figure 5.4: Closed-loop simulation for the perturbed condition ($m_2 = 10455 * 1.5\ kg$ and $\mu = 0.7$)(dotted line: the fixed-gain controller)(solid line: the gain-scheduled controller using linear interpolation)

gain-scheduled controller using linear interpolation are compared with those of a fixed-gain controller. The fixed-gain controller is designed on the operating speed of 25 m/s and uses $W_1(s) = 2$ and $W_2(s) = \frac{1}{2s+1}$, which has already been validated in experiments [42]. The simulation results for the nominal plant are shown in Figure 5.3. The dotted line is for the fixed-gain controller, and the solid line is for the gain-scheduled controller. It is shown that the transient lateral errors at three sensor locations (y_{s1}, y_{s2} and y_{s3}) are smaller for the gain-scheduled controller. Sensor 1 is placed near the front axle of the tractor, sensor 2 is placed near the rear axle of the tractor and sensor 3 is placed near the rear axle of the trailer. The simulation results for a perturbed system ($m_2 = 10455 * 1.5kg, \mu = 0.7$) are shown in Figure 5.4. Apparently, the gain-scheduled controller sustains a larger robust region. For instance, the transient oscillation of the trailer is worse when using the fixed-gain controller. Simulation on the scheduling controller using stability-preserving interpolation is compared with the controller using linear interpolation in Figure 5.5. The stability-preserving interpolation controller is using the same shaping factors $W_1(s)$ and $W_2(s)$ as what used in the linear-interpolation controller. We have $max\{\|N_{30} - N_{18}\|, \|P_{30} - P_{18}\|\} = 4.98$ and it indicates that the linear parameter-varying system will be exponentially stable if $|\dot{v}(t)| < 2.4\ m/s^2$. The upper bound is above the maximum acceleration of TSCV. As seen from the Figure 5.5, there is not much difference between these two methods, since the solutions of N_i (and P_i) are close to each other so that the stability-preserving interpolation method is close to linear interpolation method. If N_i (and P_i) are exactly equal to each other, the stability-preserving method reduces to the linear interpolation.

5.6 Conclusions

A gain-scheduled H_∞ loop-shaping controller has been designed for automated guidance of the tractor-semitrailer combination vehicle. The simulation results show that it has a larger robustness region than the fixed-gain controller, because it connects several robust regions supplied by

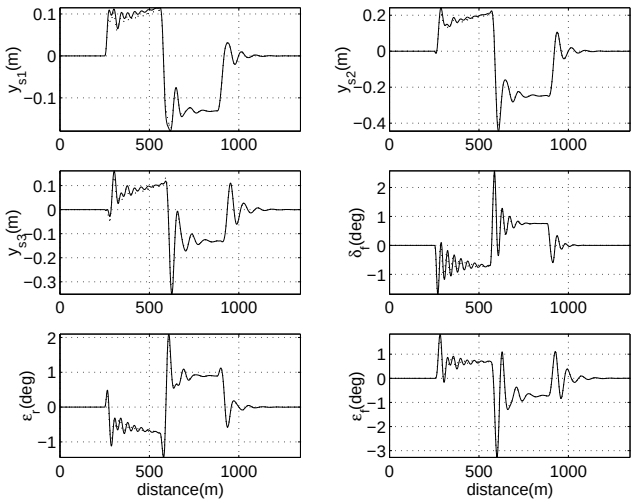

Figure 5.5: Closed-loop simulation on the perturbed condition ($m_2 = 10455 * 1.5\ kg$ and $\mu = 0.7$) for the gain-scheduled controllers using linear interpolation (dotted line) and using the stability-preserving interpolation (solid line)

different controllers which are designed for different speeds. By utilizing the vehicle speed as the scheduling parameter, the controller minimizes the effect of the uncertainties and nonlinearities, which depends mainly on the velocity, and it becomes more robust to model uncertainty. Two different scheduling techniques are also applied to the proposed controller and a very minor difference of performance is observed in simulations.

Chapter 6

LPV Controller

This chapter proposes a Linear Parameter Varying (LPV) controller design for automated lane keeping for vehicles. The lane keeping objective is to keep the vehicle centered with respect to the lane boundaries by applying appropriate steering action. Most current implementation of lane keeping controllers were based on linear synthesis techniques because linear techniques offer a direct trade-off between steering action, passenger comfort, robustness and tracking performance. However, linear methods assume constant longitudinal velocity of the vehicle for controller synthesis. It is known that the position response of the vehicle to the steering input varies significantly with the longitudinal velocity of the vehicle. The LPV design technique deals with this issue by synthesizing a velocity dependent controller. The controller minimizes the induced $\mathcal{L}_2$ norm of the closed loop from the road curvature to the tracking error. The design has been successfully implemented on a tractor semi-trailer vehicle and experiments conducted up to longitudinal velocity of 60 MPH are presented.

keywords: LPV control, automatic steering, vehicle control, tractor semi-trailer, h-infinity

6.1 Introduction

Automation of heavy vehicle operation is becoming an active area of research (Chen and Tomizuka 1995, Canudas 1998, Fritz 1999, Bruin et al. 1999, Kanellakopoulos 1999, Stepanapoulou 2000). In the context of Intelligent Transportation Systems (ITS), Automated Highway Systems (AHS) and Advanced Vehicle Control Systems (AVCS) the importance of heavy vehicles is pronounced. Profit oriented operation of heavy vehicles makes their study in the context of ITS, AHS and AVCSS commercially important. Apart from cost benefits, AVCS technologies have a strong potential to improve safety of heavy vehicle traffic by reducing driving stress on the driver.

Automatic lane guidance or lateral control is an important aspect of automating the heavy vehicle operation. Design of a lane keeping controller involves determination of the steering input that trades off best the following usual control objectives: tracking performance (how centered the vehicle is in the lane), passenger comfort (smooth lateral motion), steering action (bandwidth issue) and robustness (parameters and environment).

The challenges arise in controlling heavy vehicle lateral dynamics are:
(i) Large inertia which causes slower response to steering.
(ii) Inherent nonlinearities in the vehicle model such as the longitudinal velocity (when it is

considered an independent state of the model) and tire lateral force saturation.
(iii) Unusually large uncertainties in vehicle parameters and environmental disturbances.

Several linear and nonlinear controllers have been proposed in recent years to address the above mentioned issues in designing lateral controllers. Controllers based on back stepping, minimal induced $\mathcal{L}_2$ norm, loop shaping, input output linearization and nonlinear adaptive robust control theory have been designed (Chen and Tomizuka 1995, Wang and Tomizuka 1998, Tai and Tomizuka 1998, Hingwe and Tomizuka 1999, Bruin and Bosch 1999).

Controllers based on linear model of the vehicles have largely relied on frequency domain synthesis because various performance criteria are modeled in frequency domain effectively. For example, in frequency domain, it is intuitively easy to formulate the conflict between the tracking performance and the smoothness requirement of the input in frequency domain. However, one of the major drawbacks in using linear time invariant techniques of control design is the assumption that operating velocity is fixed. This is regardless of the fact that the vehicle dynamics are strongly dependent on velocity (Guldner et al., 1999). Therefore, to account for change in velocity, ad-hoc "gain scheduling" with respect to velocity is often practiced but the stability of the switching scheme remains questionable.

On the other hand, while nonlinear control strategies are capable of handling variation in velocity and other nonlinearities of the vehicle model, they fail to take advantage of the reality that the vehicles dynamics are closer to linear for normal highway operation. Therefore even a nonlinear controller needs to offer a good linear performance under such operating conditions. Moreover, it is difficult to incorporate passenger comfort and steering smoothness criteria explicitly in the controller design.

In recent years, the Linear Parameter Varying (LPV) control theory has gained popularity. Main advantage of the LPV methodology is in allowing application of powerful linear synthesis concepts to nonlinear systems. Researchers (Wu 1995, Wu et al. 1996) have proposed an H_∞ optimal control design technique for systems which are LPV with a rate bound on the parameter. However, the LPV synthesis theory has started finding applications only recently. In the context of lateral guidance of vehicles, a nonlinear vehicle model (with longitudinal velocity as a state of the model) becomes an LPV model when longitudinal velocity is considered as a parameter of the vehicle model. LPV synthesis methodology then allows synthesizing a single lateral controller as a function of longitudinal velocity. Several important factors like road curvature disturbance, measurement noise, actuator dynamics and the compromise between tracking performance and comfort can be incorporated in a quantitative manner in controller design.

In this chapter the LPV technique is applied to design a lane following controller for tractor semi-trailer combinations with changing velocity. The objective of the chapter is to demonstrate that the LPV design methodology allows a natural approach to solving the lane keeping problem for vehicle lateral control. To make the control problem challenging, only a single look down measurement, lateral distance of the truck from lane centerline at the front bumper, is chosen to be the input to the controller. The desired steering angle is the output of the controller. The LPV controller minimizes the induced $\mathcal{L}_2$ norm from road curvature to lateral error according to various frequency dependent weightings on the outputs and inputs as well as proper modeling of noise and disturbance. To show that LPV methodology can potentially provide better performance, it is compared with another linear design which also minimizes induced $\mathcal{L}_2$ norm for an identical formulation. Specifically, the LPV design is compared with a robust H_∞ controller. The robust controller is designed to be stable for a range of velocities. However, the stability and performance is not guaranteed if the operating velocity changes.

The chapter is organized as follows. Section 6.2 introduces the vehicle model for tractor semi-trailers and its verification. Section 6.3 discusses various issues in lateral control such as

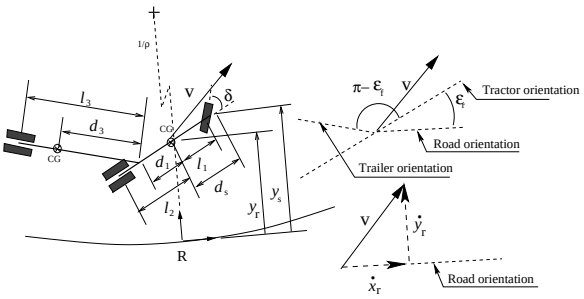

Figure 6.1: States and geometric parameters of the tractor-semi-trailer model.

design objectives, constraints and possible solutions. Section 6.4 presents problem formulation common to induced $\mathcal{L}_2$ minimization designs. Section 6.5 describes the LPV controller design methodology and its application to lateral control of tractor semi-trailers. Section 6.6 presents the comparison of the LPV controller with robust H_∞ controller. Section 6.7 describes the experimental setup and the experimental results. Section 6.8 concludes the chapter.

6.2 The vehicle model

Chen (1995) has derived dynamical equations representing lateral dynamics of a tractor semi-trailer combination. The states of the model are described relative to a "road coordinate system" which is centered at a point on the road centerline such that it is closest to the tractor center of gravity. The axes of this coordinate system are aligned along the tangent, normal and binormal to the road centerline. Under simplifying assumptions such as small relative yaw of the tractor with respect to the road, small articulation angle and small steering angle, the dynamics of the tractor semi-trailer are given by:

$$\frac{d}{dt}\begin{bmatrix} q_r \\ \dot{q}_r \end{bmatrix} = \begin{bmatrix} 0 & I \\ -M^{-1}K & -M^{-1}C \end{bmatrix}\begin{bmatrix} q_r \\ \dot{q}_r \end{bmatrix} + \begin{bmatrix} 0 \\ M^{-1}F \end{bmatrix}\delta + \begin{bmatrix} 0 \\ E_1 \end{bmatrix}\dot{\epsilon}_d + \begin{bmatrix} 0 \\ E_2 \end{bmatrix}\ddot{\epsilon}_d \tag{6.1}$$

$$y_s = \begin{bmatrix} 1 & d_s & 0 & 0 & 0 & 0 \end{bmatrix}\begin{bmatrix} q_r^T & \dot{q}_r^T \end{bmatrix}^T \tag{6.2}$$

where $q_r = [y_r,\ \epsilon_r,\ \epsilon_f]^T$ and $\dot{q}_r$ are the states of the system. y_r is the distance of the tractor center of gravity from the road centerline, ϵ_r is the yaw angle between the tractor longitudinal axis and the axis of the road coordinate system along the tangent to road centerline and ϵ_f is the articulation angle (see Fig. 1). A lateral displacement sensor (located at the front bumper of the tractor which is d_s distance ahead of the center of gravity) measures its distance from the road centerline. This measurement, is denoted by y_s, is the only measured output used for feedback. The input to the model is δ, the steering angle of the front wheel. $\dot{\epsilon}_d = v\rho$ is the angular velocity of the road coordinate system where v is the longitudinal velocity of the vehicle and ρ is the road curvature. In this chapter road curvature will be treated as a disturbance. Matrices appearing in the system equation are given below.

$$M = \begin{bmatrix} m_1+m_2 & -m_2(d_1+d_3) & -m_2d_3 \\ -m_2(d_1+d_3) & \begin{pmatrix} I_{z1}+I_{z2} \\ +m_2(d_1^2+d_3^2) \\ +2m_2d_1d_3 \end{pmatrix} & I_{z2}+m_2d_3^2 \\ -m_2d_3 & I_{z2}+m_2d_3^2+m_2d_1d_3 & I_{z2}+m_2d_3^2 \end{bmatrix}$$

$$C = \frac{2}{v}\begin{bmatrix} \begin{bmatrix} C_f+ \\ C_r+C_t \end{bmatrix} & \begin{bmatrix} l_1C_f-l_2C_r \\ -(l_3+d_1)C_t \end{bmatrix} & -l_3C_t \\ \begin{bmatrix} l_1C_f \\ -l_2C_r \\ -(l_3+d_1)C_t \end{bmatrix} & \begin{bmatrix} l_1^2C_f+l_2^2C_r \\ +(l_3+d_1)^2C_t \end{bmatrix} & \begin{bmatrix} l_3(l_3+ \\ d_1)C_t \end{bmatrix} \\ -l_3C_t & l_3(l_3+d_1)C_t & l_3^2C_t \end{bmatrix}$$

$$K = \begin{bmatrix} 0 & -2(C_f+C_r+C_t) & -2C_t \\ 0 & -2(l_1C_f-l_2C_r-(l_3+d_1)C_t) & 2(l_3+d_1)C_t \\ 0 & 2l_3C_t & 2l_3C_t \end{bmatrix}$$

$$F = 2C_f[1\ l_1\ 0]^T$$

$$E_1 = \begin{bmatrix} (-(m_1+m_2)v - \frac{2}{v}(l_1C_f-l_2C_r-(l_3+d_1)C_t)) \\ (m_2(d_1+d_3)v - \frac{2}{v}(l_1^2C_f+l_2^2C_r+(l_3+d_1)^2C_t)) \\ (m_2d_3v - \frac{2}{v}l_3(l_3+d_1)C_t) \end{bmatrix}$$

$$E_2 = \begin{bmatrix} m_2(d_1+d_3) \\ -(Iz_1+Iz_2+m_2(d_1+d_3)^2) \\ -(Iz_2+m_2d_3d_3+m_2d_1d_3) \end{bmatrix}$$

m_1 and m_2 are the mass of the tractor and the mass of semi-trailer respectively. I_{z1} and I_{z2} are the moments of inertia of the tractor and the semi-trailer respectively. $2C_{\alpha_f}$,$2C_{\alpha_r}$ and $2C_{\alpha_t}$ are the combined cornering stiffnesses of the front tires of the tractor, rear tires of the tractor and tires of the trailer respectively. Geometric parameters associated with the tractor-semi-trailer model are illustrated in Fig. 1 . Note that the Matrix C depends on velocity v, making the model LPV.

6.2.1 Model verification

The parameters for model in Eq. (6.1) were obtained by tuning the parameters to fit experimantal frequency response. Sinusoidal excitation of different frequencies was given to the steering wheel at constant speed of 20, 40 and 60 miles per hour. The lateral acceleration response to steering input, $\ddot{y}_s$, was measured. Figure 2 shows the measured lateral acceleration response (discrete dots). The parameters given in Table 6.1 gave a sufficiently good fit to the measured data. The model, shown as dash-dot, solid and dashed lines in Fig. 2 , denotes transfer function from steering angle to lateral acceleration at 20, 40 and 60 MPH respectively. For all three speeds, the match between the "tuned" model and the data is good at frequencies below 1 Hz. At higher frequencies, the discrepancy is likely to be the result of tractor suspension (Feng and Tan, 1999). The closed loop bandwidth for the truck is expected to be less than 1 Hz because of large weight to lateral force ratio. Therefore the model is adequate for control design purposes.

6.2.2 Remarks on vehicle dynamics

1. Equation (6.1) is derived from a nonlinear model assuming small relative yaw, small articulation angle and small steering angle. Moreover, it assumes a constant longitudinal velocity. If this assumption is removed, then terms with longitudinal acceleration will

Table 6.1: Model parameters

Description	value
Mass of the tractor, m_1	7727 kg
Mass of the trailer, m_2	10455 kg
Tractor yaw moment of inertia, I_{z1}	45926 kgm^2
Trailer yaw moment of inertia, I_{z2}	161780 kgm^2
Tractor front tire cornering stiffness, C_{α_f}	180,000 N/rad
Tractor rear tire cornering stiffness, C_{α_r}	325,000 N/rad
Trailer tire cornering stiffness, C_{α_t}	325,000 N/rad
Distance of tractor front axle from tractor CG, l_1	1.6 m
Distance of rear tractor axle from tractor CG, l_2	3.745 m
Distance of trailer axle from king pin, l_3	6.5 m
Distance of king pin from tractor CG, d_1	3.24 m
Distance of trailer CG from king pin, d_3	3.8 m
Distance of lateral error sensor ahead of the tractor CG, d_s	2.00 m

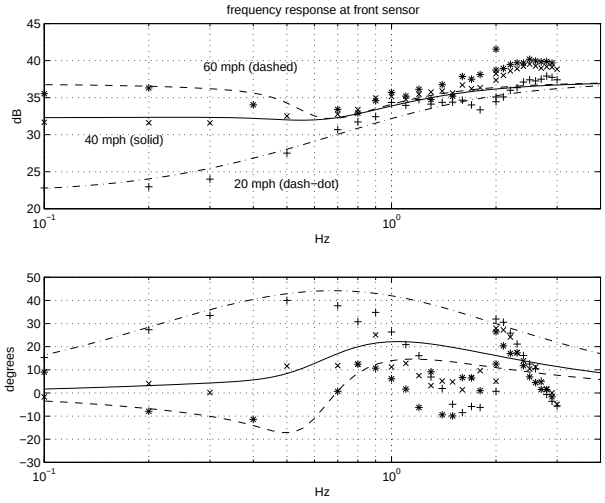

Figure 6.2: Frequency response of the tractor semi-trailer from δ to $\ddot{y}_s$

appear in the right hand side of Eq. (6.1). However, these terms are small and will be considered as disturbances to the lateral dynamics (in he same way as road curvature is considered as a disturbance).

2. A combined lateral and longitudinal model of the vehicle will include the longitudinal velocity of the vehicle as a state. In this case, the model becomes nonlinear with the longitudinal velocity as one of the dominant source of nonlinearity. One way to decouple the lateral and longitudinal dynamics is to assume longitudinal velocity as a parameter to the lateral dynamics. This is the approach taken in the chapter.

3. Several lateral disturbances like the wind and super-elevation can be clubbed together with the curvature disturbance which is the largest disturbance in practice when no a-priory information about the road curvature is available to the controller.

4. The model in Eq. (6.1) excludes the steering actuator. The bandwidth and the power of the steering actuator will influence the achievable closed loop performance. Therefore, steering actuator dynamics need to be included for controller design. A model of the steering actuator has been approximated (Hingwe et al., 1999) and will be included at the control design stage.

6.3 Control objective, design constraints and control strategies

In terms of the model given by Eq. (6.1), the basic control objective is to keep the lateral error y_s small in face of road curvature disturbance ρ using the steering angle δ as the control input. This simple criteria is not a sufficient description of the control objective in any practical vehicle control implementation. A comprehensive discussion of control requirements and constraints associated with vehicle steering control is presented in the subsection that follows. Some control strategies are reviewed and motivation for LPV design is discussed.

6.3.1 Remarks on controller requirements

- Dynamic tracking requirement of the lane center: The tracking performance can be either specified in time or frequency domain. The time domain tracking performance specification can be done in terms of the maximum transient error to a step change in road curvature and the steady state tracking error. In frequency domain, tolerable error as a function of frequency, which includes steady state error, can be specified. Simplistic specification of the tracking error performance may be insuficient and lead to a bad controller design.

- Smoothness of steering action: Any chatter in the steering command could reduce the life of the mechanical components of the actuator without corresponding control benefits. Thus, the steering effort for lateral control should be smooth.

- Passenger comfort: This is not a well defined requirement and is related to peak lateral acceleration by many researchers. In practice, this may be addressed by providing enough damping to various vehicle and actuator modes.

- Well Damped internal dynamics: Road vehicles are generally under-actuated in the sense that only one input (steering) is available to control both the lateral dynamics and the yaw

dynamics. In the case of tractor a semi-trailer, this problem is augmented by the possibility of articulation angle instability (jack-knifing). It can be shown that if the control objective is to regulate the lateral error y_s, then the yaw dynamics of the tractor and the trailer become the internal dynamics of the closed loop system. Although these dynamics are usually stable, enough damping should be designed to handle the possibility when these dynamics are severely under damped (e.g. low road adhesion and/or high velocity).

- Robustness to parametric uncertainties: The vehicle dynamics depend on several parameters. Geometric parameters such as the wheel base, location of the fifth wheel and distance of the trailer axle from the fifth wheel are measurable. Inertial parameters like mass and moments of inertia can vary over a wide range depending on the load in the trailer. Friction parameters arising from tire-road friction properties can be uncertain and vary suddenly (because of spilled oil, ice patch, wet pavement etc). These variations and uncertainties pose a formidable challenge to the control design.

The above control design objectives have to be achieved amidst practical constraints some of which are given below.

6.3.2 Measurements and actuator

- Control design is always constrained by the availability and quality of measurements. In consonance with the goal of lateral guidance, the common measurements assumed for lateral control design are: (i) Tracking error (ii) Yaw rates and (iii) Acceleration. The tracking error is obtained by a road reference system. Two popular road reference systems are (i) Machine vision based and (ii) Magnetic marker based. The vision system can provide a lot of road information ahead of the vehicle but its reliability in inclement weather is questionable. The magnetic marker based system is accurate and reliable but is a look down system and does not see the road ahead of the vehicle. The look down system makes the control problem more challenging as compared to vision based system which provides a look-ahead. To alleviate this drawback, two look down measurements, one in the front of the vehicle and the other at the back, have been used to generate a virtual look ahead displacement. Other sensors that can be used for steering control are yaw rate sensors and accelerometers but these sensors are plagued with significant noise. Irrespective of the number of measurements used in the control design, issue of noise in measurements needs to be addressed.

- The model in Eq. (6.1) does not specify actuator dynamics. Therefore, it allows for unrealistically high performance to be achieved. In practice, the steering actuator has limited bandwidth and power. Therefore, it is crucial to penalize such high demand steering action which is also harmful to actuator life.

Several control strategies have been proposed to take care of some of the above control objectives and constraints. However, most of them have some limitations.

6.3.3 Preview of control strategies

Nonlinear control

Some nonlinear control strategies like Sliding Mode Control (SMC) and Adaptive Robust Control (ARC) have been applied to the problem of steering control of tractor semi-trailers (Tai and

Tomizuka, 1999). The nonlinear control strategies address lateral and longitudinal dynamics coupling naturally. Controllers like SMC are robust to parametric uncertainties. However, the high gain and control chatter is often detrimental to actuator wear and passenger comfort. Chatter has been dealt with effectively in literature by introducing a boundary layer around the sliding surface, where the control is smooth (Slotine and Li, 1991), or by addition of an integrator to the input of the vehicle. The performance objective in nonlinear control designs like SMC is often regulation of the tracking error. In the face of this objective, the yaw dynamics become the internal dynamics of the closed loop system. It has been shown that for passenger cars, the damping of the yaw internal dynamics decreases as the velocity increases (Hingwe and Tomizuka, 1998). A velocity dependent look-ahead as been proposed to keep the yaw dynamics well damped. Unfortunately, long look ahead displacement, when estimated using look down measurements, contains amplified noise from the look down measurements. Furthermore, typical nonlinear strategies are state feedback. There is no direct measurement for states like lateral velocity $\dot{y}_r$. Measurement of other states require additional sensors such as yaw rate and articulation angle sensor. Because the vehicle nominally operates around small values of yaw rate and articulation angles, the measurements from these sensors have high noise to signal ratio. Filtering, if used, has to be done in a way such that the stability can be guaranteed. The use of estimators or observers for lateral velocity compounds the proof of stability further.

Linear control

Various linear controllers have been proposed in the literature for application to the steering control of tractor semi-trailer vehicles. The main motivation for considering linear control design for vehicle lateral control is that vehicle dynamics have been observed to be linear for fixed operating velocity and small steering inputs. This is the typical operating region for a vehicle on highways. Furthermore, the compromise between tracking accuracy, ride comfort and smoothness of steering action is relatively easy to formulate in frequency domain. A Frequency Shaped Linear Quadratic (FSLQ) controller was one of the earlier such controllers (Peng and Tomizuka, 1993) applied to lateral control of passenger cars. For tractor semi-trailers, manual loop shaped and optimal H_∞ loop shaped controllers have been tested (Wang et al. 1999, Hingwe et al., 1999). However, these controllers were designed with the assumption that the operating velocity is fixed. Nevertheless, these controllers can be analyzed for stability under varying velocity conditions by a Lyapunov function analysis which relaxes the constant velocity assumption and assumes a bound on the acceleration. In lieu of the Lyapunov function, extensive simulations can be performed. In any case, the performance requirement across different velocities is not specified at the design stage. Moreover, design of velocity independent controllers which are stabilizing for a range of velocities may be a very conservative approach which fails to utilize the change in vehicle dynamics with velocity.

The speed dependent characteristic of the steering control problem is demonstrated by a classical frequency domain synthesis applied to the identified truck semi-trailer model in Fig. 2 . Assume that lateral error at the front bumper (y_s) is the only measurement available for feedback. From the frequency response of lateral acceleration to steering angle (Fig. 2), it can be seen that a proportional controller will stabilize the vehicle at 20MPH if the gain is such that the open-loop frequency crossover point is around 0.4 Hz. As the velocity increases, the gain crossover will move towards higher frequency and the phase margin will decrease. Therefore, a proportional controller will be inadequate for stability at high speed. A compensator which adds phase at the target gain crossover is required. The phase lead requirement increases with increase in velocity making the control design challenging. The compensator should also be

able to attenuate high frequency measurement noise for smooth control action. It can be seen from Fig. 2 that low frequency gain of the vehicle increases with velocity. This suggests that the controller can afford to have a lower "low frequency gain" as the velocity increases. This possibility of adjusting the low frequency gain as a function of velocity provides crucial freedom to add mid frequency phase to the compensator while keeping the high frequency noise attenuation at a constant level. Therefore, it is of fundamental interest to incorporate such "gain scheduling" in the design of lateral controller to achieve high performance lateral guidance systems.

6.3.4 Proposed strategy

The conventional meaning of "gain scheduling" has implied designing different controllers, each at a particular value of a parameter, and interpolating between the controllers as the parameter value changes. This does not guarantee stability always and does not incorporate the rate of the parameter change in the design. A methodology which promises to help design the required velocity dependent controller is the LPV design technique. The design is an induced $\mathcal{L}_2$ minimization admitting performance specification in frequency domain. Therefore frequency based ideas of stability, performance and robustness (as used popularly in μ synthesis) are applicable directly. Moreover, the methodology allows specification of velocity dependent performance objective. The maximum acceleration and deceleration capability of the vehicle at different speed is also naturally incorporated in the design specification. A single controller which is a continuous function of velocity and guarantees to achieve certain performance over a velocity range is the output of the design exercise. The objective of the rest of the chapter is to formulate an appropriate LPV design and show that is is an effective method for designing a lane guidance controller. It will be shown that the much required phase lead in mid frequencies is added by the LPV methodology by taking advantage of the variation in vehicle dynamics with respect to velocity.

There are more ways than one to add the mid frequency phase lead to the compensator such as "virtual look ahead" feedback using lateral error measurements from the front as well as the back of the vehicle or incorporating yaw rate feedback. However, by observing the frequency response given in Fig. 2 ,it can be concluded that front lateral error sensor alone is capable of providing the required lead. Since the purpose of this chapter is to demonstrate the feasibility and appropriateness of the LPV methodology to tractor semi-trailers, the problem is made more challenging by limiting the feedback to the lateral error measured at the front end of the vehicle.

The solution generated by the LPV methodology is as good as the problem formulation and performance specification. In the next Section, problem formulation with emphasis on performance specification will be presented. The formulation will not be specific to LPV design methodology but will be admissible to any induced $\mathcal{L}_2$ design methodology. This formulation allows for fair comparison between LPV and robust Linear Time Invariant (LTI) controllers.

6.4 Problem formulation for tractor semi-trailer vehicles

Although the main motivation of this chapter is to study the LPV design for tractor semi-trailer, the LPV design will be compared to another design which is H_∞ optimal. Specifically, an H_∞ LTI controller which is robust to a range of velocities will be designed using the μ synthesis. This warrants a Linear Fractional Transform (LFT) representation of the system. An LFT representation is not required for the LPV synthesis but will be used to preserve the similarity of the problem formulation for different designs.

In the next subsection, the LFT formulation will be described.

6.4.1 Vehicle model as a LFT over velocity

In this subsection the vehicle dynamics are written as an LFT of an LTI system over velocity. Because velocity appears as rational function in Eq. (6.1), it can always be represented as an LFT of an LTI system over velocity. For convenience, we use a normalized representation of longitudinal velocity given by

$$v = v_n + \beta w_v \tag{6.3}$$

where v_n and w_v are fixed numbers and β is a variable denoting normalized velocity. For example, $v_n = 20$, $w_v = 10$ and $\beta \in [-1 \quad 1]$ means velocity $v \in [10 \quad 30] m/s$.

Consider the following static relations:

$$\begin{bmatrix} \eta_i \\ z_i \end{bmatrix} = \begin{bmatrix} \frac{1}{v_n} & -\frac{w_v}{v_n^2} \\ 1 & -\frac{w_v}{v_n} \end{bmatrix} \begin{bmatrix} \xi_i \\ w_i \end{bmatrix} \qquad i = 1, 2, 3 \tag{6.4}$$

and

$$w_i = \beta z_i \qquad i = 1, 2, 3 \tag{6.5}$$

It can be verified that substituting Eq (6.5) in Eq. (6.4) gives

$$\eta_i = \frac{\xi_i}{v_n + \beta w_v} \qquad i = 1 \ldots 3 \tag{6.6}$$

Thus Eqs. (6.5) and (6.4) are an LFT representation of Eq. (6.6).

Next, consider the following dynamic system

$$\begin{bmatrix} \dot{q}_r \\ \ddot{q}_r \\ \mathbf{w} \\ e \\ y \end{bmatrix} = \begin{bmatrix} \mathbf{0} & I & \mathbf{0} & \mathbf{0} & \mathbf{0} \\ -M^{-1}K & \mathbf{0} & I & M^{-1}E_1 & M^{-1}F \\ \mathbf{0} & -M^{-1}D^* & \mathbf{0} & \mathbf{0} & \mathbf{0} \\ C_1 & \mathbf{0} & \mathbf{0} & D_{11} & D_{12} \\ C_2 & 0 & 0 & D_{21} & D_{22} \end{bmatrix} \begin{bmatrix} q_r \\ \dot{q}_r \\ \mathbf{z} \\ \rho \\ \delta \end{bmatrix} \tag{6.7}$$

where $\mathbf{w} = [\ w_1 \quad w_2 \quad w_3\ ]^T$ $\mathbf{z} = [\ z_1 \quad z_2 \quad z_3\ ]^T$,

$$\frac{D^*}{2} = \begin{bmatrix} \begin{bmatrix} C_f + \\ C_r + C_t \end{bmatrix} & \begin{bmatrix} l_1 C_f - l_2 C_r \\ -(l_3 + d_1) C_t \end{bmatrix} & -l_3 C_t \\ \begin{bmatrix} l_1 C_f \\ -l_2 C_r \\ -(l_3 + d_1) C_t \end{bmatrix} & \begin{bmatrix} l_1^2 C_f + l_2^2 C_r \\ +(l_3 + d_1)^2 C_t \end{bmatrix} & \begin{bmatrix} l_3(l_3 \\ +d_1) C_t \end{bmatrix} \\ -l_3 C_t & l_3(l_3 + d_1) C_t & l_3^2 C_t \end{bmatrix}$$

$C_1 = \begin{bmatrix} 1 & d_s & 0 \\ 0 & 0 & 0 \end{bmatrix}$, $C_2 = [\ 1 \quad d_s \quad 0\ ]$, $D_{11} = \begin{bmatrix} 0 \\ 0 \end{bmatrix}$,
$D_{12} = \begin{bmatrix} 0 \\ 1 \end{bmatrix}$, $D_{21} = 0$ and $D_{22} = 0$.

It is easy to see that Eqs. (6.4), (6.5) and (6.7) define an LFT representation of the model in Eq. (6.1) over normalized velocity β. This representation is shown in Fig. 3 compactly. P in Fig. 3 is the constant matrix in the right hand side of Eq. (6.7). Error e in Eq. (6.7)is $[y_s,\ \delta]$, the output y is y_s. The inputs are δ, the steering angle of the road wheel and ρ, the road curvature. The goal of this formulation is to design a feedback controller around y_s and δ (see Fig. 3) such that the effect of disturbances like ρ on error e is minimized. Notice that including control effort δ in the definition of error allows specification of the compromise between tracking accuracy and smoothness of steering action.

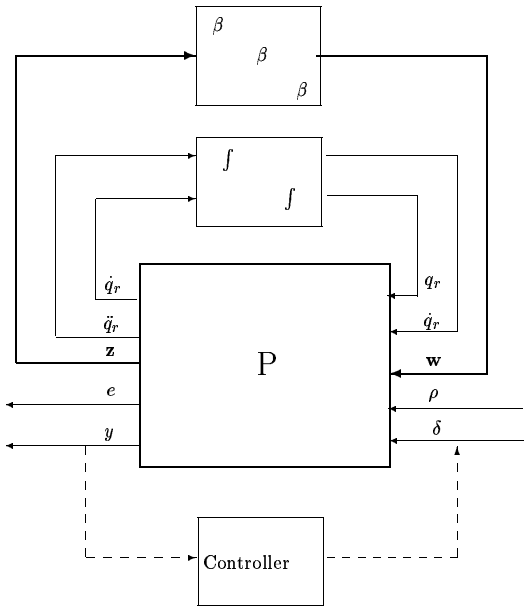

Figure 6.3: LFT representation of the tractor semi-trailer model

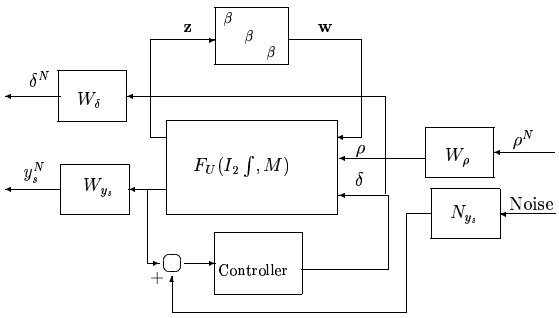

Figure 6.4: Performance weight specification

To include some of the controller requirements and practical constraints in the design, measurement noise, disturbance models and performance specification are added to the LFT model as shown in Fig. 4 . In this figure, W_ρ and N_{y_s} are road disturbance and noise models respectively. W_δ and W_{y_s} are the performance weights on steering action and lateral error. Frequency shaping is used in specifying these performance weights and is explained in the following subsections.

Disturbance modeling

As mentioned before, the road curvature ρ is the most dominant lateral disturbance. A maximum curvature disturbance of $\frac{1}{400}1/m$ is assumed (this is a harsh disturbance at highway speeds). The road disturbance model is assumed to be a low pass filter at 1 Hz because the road curvature does not change frequently on highways and truck lateral bandwidth is less than 1 Hz. The following disturbance model approximates the allowable disturbances.

$$W_\rho = \frac{1}{400}\frac{(s^2+2\xi_1\omega_1 s+\omega_1^2)}{(s^2+2\xi_2\omega_2 s+\omega_2^2)}\frac{(\omega_2^2)}{(\omega_1^2)} \tag{6.8}$$

where $\omega_1 = 20\pi$, $\xi_1 = 0.7$, $\omega_2 = 2\pi$ and $\xi_2 = 0.7$. Thus, all allowable $\mathcal{L}_2$ signals (ρ^N) are filtered by W_ρ to result in signals ρ, which model low frequency disturbances.

Penalty on lateral error y_s

The high frequency component of lateral error measurement is considered noise. This is because the vehicle dynamics are slow and the road curvature is piecewise constant. Therefore, the penalty on lateral error is set high only on the low frequency content of the lateral error measurement as given by

$$W_{y_s} = \frac{1}{2}\frac{(s+0.2\pi)}{(s+0.004\pi)} \tag{6.9}$$

Penalty on steering action

The optimization problem is ill posed until a penalty on the control effort (the steering action) is imposed. Further, high frequency movements of the steering have to be restricted because (1) the actuator may saturate (2) the mechanical components may not survive the high frequency chatter. The following transfer function reflects the above considerations

$$W_\delta = \frac{5}{1}\frac{(s^2+2\xi_1\omega_1 s+\omega_1^2)}{(s^2+2\xi_2\omega_2 s+\omega_2^2)}\frac{(\omega_2^2)}{(\omega_1^2)} \tag{6.10}$$

where $\omega_1 = \pi$, $\xi_1 = 0.7$, $\omega_2 = 200\pi$ and $\xi_2 = 0.7$. This penalty allows for a maximum of 11.5 degrees of tire steering angle at frequencies lower than 0.1 Hz whereas the allowable tire steering angle at 2 Hz is .36 degrees (equal to about 7.6 degrees of the steering wheel in the cabin).

Noise in measurement of y_s

It is assumed that the lateral error measurement is obtained from magnetic markers embedded in the center of the lane. The lateral error is updated when the vehicle passes over a magnet and is held at the previous value otherwise. The distance between consecutive magnets is typically one meter. There are two sources of noise in the measurement which emanate from this scheme. One source of noise is from holding the position measurement obtained from a magnet until a new magnet is encountered by the vehicle. This noise has frequencies equal to the update frequency and higher harmonics. Another source of noise is the error in placing the magnet along the ideal lane centerline and the measurement errors of the magnetic field sensors. For analysis, we can assume that the placement error includes magnetic sensor measurement error. If a 2 cm placement error is assumed in placing individual magnet along the road centerline and vehicle is moving at v m/s, then the worst case noise at v Hz is of amplitude 0.02 m. Also, it

is assumed that the mean "placement error" for an infinite sequence of magnets is zero. The placement error for a segment of length L meters is assumed linearly interpolated between zero error for $L \to \infty$ and $2cm$ error for length of one meter (distance between consecutive magnets). Therefore, the placement error for a segment of length L is $0.02/L$. In the frequency domain, this noise model can be defined as $N_{y_s}(j\omega) := \frac{j\omega}{100v\pi}$, where ω is the frequency of noise. A transfer function realization of this model is given by $N_{y_s}(s) = \frac{s}{100v\pi}$. This is approximated as a transfer function of zero relative degree (at $v = 10m/s$) by

$$N_{y_s} = 0.2\frac{s + 0.002\pi}{s + 200\pi} \tag{6.11}$$

The noise model that arises from hold operation can be verified to have the peak of $2cm$ at vm/s and then a slope of -20 dB/decade. It can be verified that Eq.(6.11) is an upper bound on this noise as well.

Steering actuator model

Steering actuator for the experimental vehicle in consideration has been designed (Hingwe et al. 1998). It is approximated as a second order low pass filter with 4 Hz bandwidth.

$$A = \frac{(6\pi)^2}{s^2 + 2(0.7)(6\pi)s + (6\pi)^2}$$

We can now restate the control objective as designing a *Controller* such that the closed loop is stable and the induced $\mathcal{L}_2$ norm from normalized disturbance $[\rho^N \; Noise]$ to normalized error $[y_s^N \; \delta^N]$ is minimized. The induced $\mathcal{L}_2$ norm of the stable closed loop system will be denoted by γ. $\gamma \leq 1$ will mean that all the performance specifications have been satisfied. The formulation is open to several induced $\mathcal{L}_2$ designs. First, we will describe and design LPV controller.

6.5 Linear Parameter Varying (LPV) Control

The output feedback LPV control synthesis result with a rate bound on the parameters is given in Wu et al. (1996).

Consider an open loop system as follows

$$\begin{bmatrix} \dot{x}(t) \\ e_1(t) \\ e_2(t) \\ y(t) \end{bmatrix} = \begin{bmatrix} A(p(t)) & B_{11}(p(t)) & B_{12}(p(t)) & B_2(p(t)) \\ C_{11}(p(t)) & 0 & 0 & 0 \\ C_{12}(p(t)) & 0 & 0 & D_{12}(p(t)) \\ C_2(p(t)) & 0 & D_{21}(p(t)) & D_{22}(p(t)) \end{bmatrix} \begin{bmatrix} x(t) \\ d_1(t) \\ d_2(t) \\ u(t) \end{bmatrix} \tag{6.12}$$

where e_1 and e_2 are errors, y is the output, x is the state, d_1, d_2 are disturbances and u is the control input. The time varying parameter, $p(t)$ takes values in compact set $\mathcal{P} \subset \mathbf{R}^m$ such that $\underline{\nu}_i(p) < \dot{p}_i \leq \overline{\nu}_i(p)$ is satisfied.

It can be seen that this problem formulation fits the open loop system illustrated in Fig. 4 where $e_1 = y_s^N$, $e_2 = \delta^N$ $y = y_s + \text{Noise}$, $d_1 = \rho$, $d_2 = \text{Noise}$, $\dot{x} = [\; q_r^T \quad \dot{q}_r^T \;]^T$, $u = \delta$ and parameter $p = v$. The bound on p is the maximum acceleration and deceleration bound on velocity.

Under the assumptions (i) $D_{22} = 0$ (This means that there is no feed-through of the steering input to the lateral error measurement)
(ii) D_{12} has full column rank (This means that the steering action is penalized along with the lateral error)
(iii) D_{21} has full row rank (This means that the lateral error measurement has noise)

some minor regularization and normalization can be done. Thus, without loss of generality, $D_{12} = I$ and $D_{21} = I$ can be assumed. Under these assumptions:

Theorem 1 (Output- feedback) *(Wu, 1995) Given a compact set $\mathcal{P} \subset \mathbf{R}^s$, performance level $\gamma > 0$ and LPV system (Eq. (6.12) with some normalization and regularization), the parameter dependent γ performance problem is solvable iff there exist matrix functions $X \in \mathcal{C}^1$ and $Y \in \mathcal{C}^1$ such that for all $p(t) \in \mathcal{P}, X(p) > 0, Y(p) > 0$ and*

$$\begin{bmatrix} -\sum_{i=1}^{m} \overline{\nu_i} \frac{\partial X}{\partial p_i} + \hat{A}X + X\hat{A}^T - B_2 B_2^T & XC_{11}^T & \gamma^{-1}B_1 \\ C_{11}X & -I & 0 \\ \gamma^{-1}B_1^T & 0 & I \end{bmatrix} < 0 \tag{6.13}$$

$$\begin{bmatrix} -\sum_{i=1}^{m} \overline{\nu_i} \frac{\partial Y}{\partial p_i} + \tilde{A}Y + Y\tilde{A}^T - C_2 C_2^T & YB_{11} & \gamma^{-1}C_1^T \\ B_{11}^T Y & -I & 0 \\ \gamma^{-1}C_1 & 0 & -I \end{bmatrix} < 0 \tag{6.14}$$

$$\begin{bmatrix} X & \gamma^{-1}I \\ \gamma^{-1}I & Y \end{bmatrix} \geq 0 \tag{6.15}$$

where $\hat{A} := A - B_2 C_{12}$ and $\tilde{A} := A - B_{12} C_2$. If these conditions are satisfied simultaneously for all combinations of $\overline{\nu_i}$, then a stabilizing controller (Wu, [8]) which achieves disturbance to error norm less than γ can be written down. The controller formula is written in terms of the system matrices and the solution to the LMI's (6.13) - (6.15). Note that solution of LMI's given by Eq. (6.13) - (6.15) involves search over infinite dimension spaces of $X(p)'s$ and $Y(p)'s$. Several approaches to solving the LMI's in Eq. (6.13) - (6.15) have been proposed. One way is to use a finite basis to represent the space of positive definite parameter dependent matrices. For example, basis $[1\, p\, p^2 \ldots p^n]$ can be used to approximate infinite dimensional space to which $X(p)$ and $Y(p)$ belong. Furthermore, gridding of the LMI's in parameter space is done. This leads to a suboptimal solution. While there is no guideline for choice of basis function and gridding, there is a compromise between optimality of solution (or even validity in case of coarse gridding in parameter space) and the computation time required. The LMI's in Eq. (6.13) - (6.15) can be transformed to LMI's involving γ^2. The γ minimization problem can be posed as a γ^2 minimization resulting in the following problem to solve

$$\min_{p \in \mathcal{P} X(p) > 0, Y(p) > 0, \gamma > 0} \gamma^2$$

6.5.1 Synthesis of LPV for tractor semi-trailers

For synthesis of the output feedback controller (finding $X(v) > 0$, $Y(v) > 0$ and performing γ^2 minimization), the velocity is assumed to be constrained by $8.89 \leq v \leq 26.66 m/s$. The acceleration/deceleration is assumed to be given by $-2.22 < \dot{v} \leq 0.533 - 0.04(v - 17.77)$ This means that the maximum deceleration is $-2.22 m/s^2$ at all velocities. The maximum possible acceleration is a function of velocity. It is $0.89 m/s^2$ at $20 mph$ and $0.18 m/s^2$ at $60 mph$. This represents more than moderate longitudinal maneuvers. The basis function chosen for $X(v)$ and $Y(v)$ were 1, v and v^2. The γ^2 minimization was performed with 15 grid points for parameter v. The order of the resulting controller was sixteen (total order of states in $P(v)$ plus states in weighting functions). Figure 5 shows the bode plot of the LPV controllers at 20 30 40 50 and 60 MPH. The magnitude plot is labeled with values of β corresponding to 20, 30, 40, 50 and 60 MPH. The dark solid line (labeled 1) is the frequency response of the controller at 60 MPH. It has phase lead action around 4 rad/s. This is achieved by a lag-lead action which introduces lower gain at low frequencies (0.2 rad/s) as compared to the plots for lower speeds (labeled by -1 corresponding to 20 MPH, 0 corresponding to 40 MPH etc.). The low gain at low frequency at high speed is acceptable because the vehicle low frequency gain at high velocity is high.

In the next Section, we present the synthesis of a robust H_∞ controller.

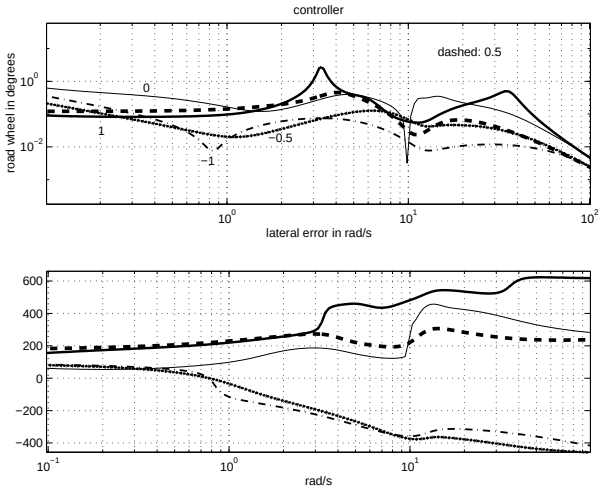

Figure 6.5: LPV designs

6.6 Robust H_∞ controller design

Another approach to designing a controller which is stable for a range of velocity is to design a robust H_∞ controller. Such controller is not guaranteed to be stable for changing speed. However, in practice, the velocities not a fast changing parameter and because of continuity properties of stability, the controller may be stable in face of changing velocity. Moreover, for vehicle lateral control, a controller designed to stabilize at higher speed is usually stable for lower speeds but the performance may be poorer. To demonstrate this point, a controller based on μ synthesis and D-K iteration is designed. The controller is designed to be stable for a range of velocity given by

$$v = v_n + \beta w_v \qquad \beta \in [-1\ 1]$$

For fair comparison with the LPV controller, the problem formulation for robust H_∞ is kept identical to the one used for the LPV synthesis. The design objective is to synthesize a constant controller K, such that the induced $\mathcal{L}_2$ norm from [δ^N Noise] to [y_s^N δ^N] (denoted by γ) is minimized. The γ minimization objective is written down as finding a stabilizing controller K (Fig. 4) such that

$$\min_{K,\beta\in[\ -1\quad 1\ ]} ||F_u[F_l(F_u(I_2 \int, P), K), \beta I_3]||_\infty \tag{6.16}$$

where $F_u(.,.)$ and $F_l(.,.)$ represent the upper and lower redheffer products, P is defined in Eq. (6.7) and K is illustrated in Fig. 4 .

$\beta \in [-1\ 1]$ represents range in velocity from 20MPH to 60MPH with 40MPH as the nominal velocity. The design is done using Matlab's *dkitgui* function. Five automatic iterations were performed. The minimum value of γ achieved was 1.469. The frequency response of the minimizing controller is given in Fig. 6 .

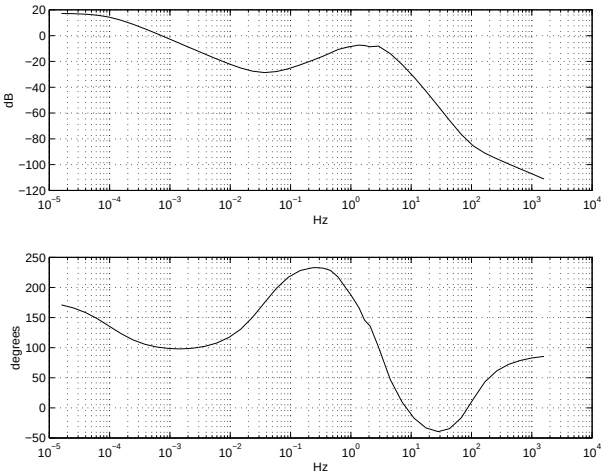

Figure 6.6: Robust $H\infty$ design

6.7 Experimental Results

6.7.1 Setup

A Freightliner FLD 120 tractor and a 45 feet Great Dane trailer equipped with sensors and actuators for lateral control were used to implement the controllers. Figure 7 gives the location and description of the sensors and actuators on the tractor and semi-trailer combination. The magnetometer array located under the front bumper of the tractor was used to measure the lateral error y_s. The measurement gets updated every time the array passes over a magnet where it is held until further update. This signal is the input to the controllers. The output of the controller is the desired steering angle and is effected by the steering actuator mounted on the steering column.

6.7.2 Digital implementation of controllers

A fourth order Runge-Kutta integration subroutine with sample time of 20 ms was used to implement all the controllers. The LPV controller is fairly complicated (computationally) function of $X(p)$ and $Y(p)$ to be evaluated in real time for changing parameter p. Therefore, it is evaluated off-line at several velocities. In particular, the LPV controller $K(v)$ was gridded into fifteen points. The gridding generated a 15 point representation given by $K(v_i) = \{A_k(v_i)\ B_k(v_i)\ C_k(v_i)\ D_k(v_i)\}, i = 1 \ldots 15$ with $i = 1$ corresponding to 20MPH and $i = 15$ corresponding to 60MPH velocity. At intermediate velocities, linear interpolation of A_k, B_k, C_k and D_k was used. The Robust H_∞ controller was also implemented in state space form using the Runge Kutta integration.

6.7.3 Closed loop results

Closed lop tests for lateral control were conducted at the Crows Landing test site illustrated in Figure 8 . The tests started from rest at the end point of the track. speed of the vehicle was controlled manually. Maximum speed achieved on the track was about 65 MPH. The braking

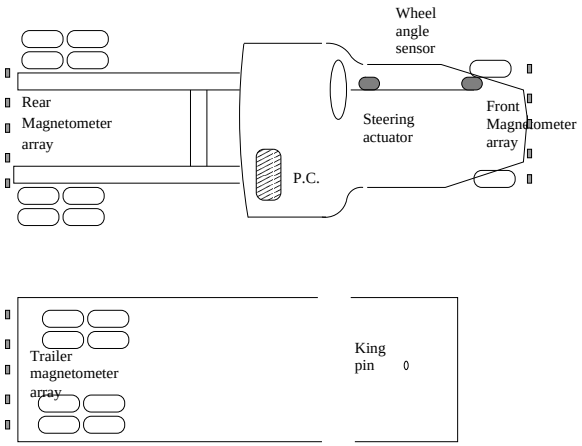

Figure 6.7: Sensors and actuators for vehicle lateral control

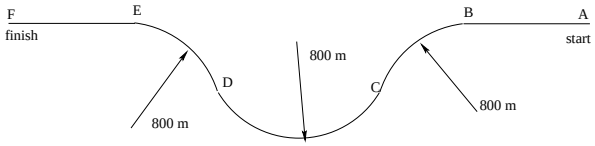

Figure 6.8: Test track at Crows Landing

required to stop the truck at the end of the track was more than moderate. It can be seen that the maximum curve transition is equivalent to $400m$ change in radius (no super-elevation to aid in steering) at points C and D on the test track in Fig. 5.

Figures 9 and 10 show the result of a typical closed loop test with the LPV controller. The velocity of the truck was controlled manually and is shown in the upper plot of Fig. 9 . Bottom plot in Fig. 9 shows the lateral error y_s measured during experiments (solid line) and one obtained during simulation (dashed line). It can be seen that the steady state errors were less than 0.1 m but the transient errors were as high as 0.6 m. Simulations were performed using the linear model. The velocity profile in Fig. 9 was used as input to the simulation. The curvature as shown in the bottom plot of Fig 10 was used as a disturbance in simulation. Note that the initial transients were a result on non zero initial conditions (tractor was not aligned properly along the track). The upper plot in Fig. 10 shows the hand wheel steering angle in degrees as measured during experiments (solid line) and as obtained by simulation (dashed line).

The closed loop results with the robust H_∞ controller are shown in Fig. 11 and 12 . the transient lateral error at points C and D on the track are as large as 0.7 m and are larger than the errors measured with the LPV controller. Also, the speed of the vehicle is only about 45 MPH. experiments at higher speed with the robust H_∞ controller were not conducted because the range of the lateral error measurements is limited to 0.8 cm on either side of the lane centerline. The solid lines in the figures correspond to the experimental data whereas the dashed lines correspond to simulations.

From these figures, it can be seen that the simulations performed on linear model are adequate for capturing the low frequency behavior but do not capture all the dynamics of the real system.

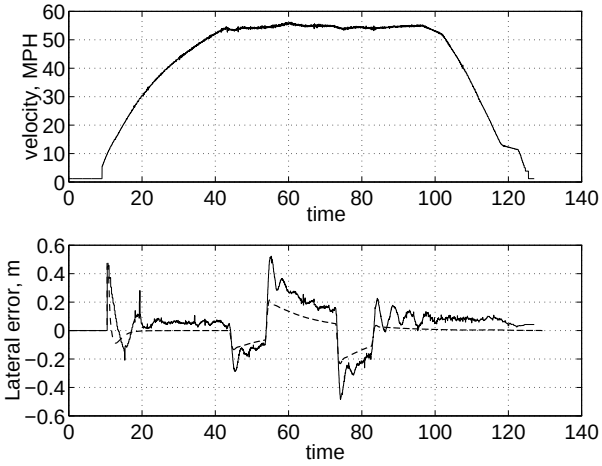

Figure 6.9: Velocity profile of the vehicle and lateral tracking error (time in sec) with LPV controller

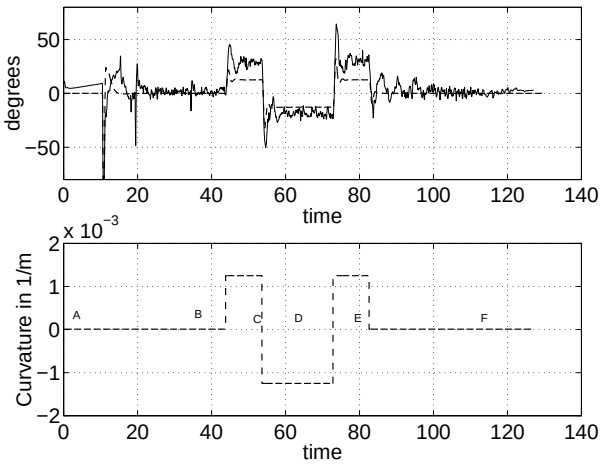

Figure 6.10: Steering wheel action measured in cabin and curvature profile used in the simulation (time in sec) with LPV controller

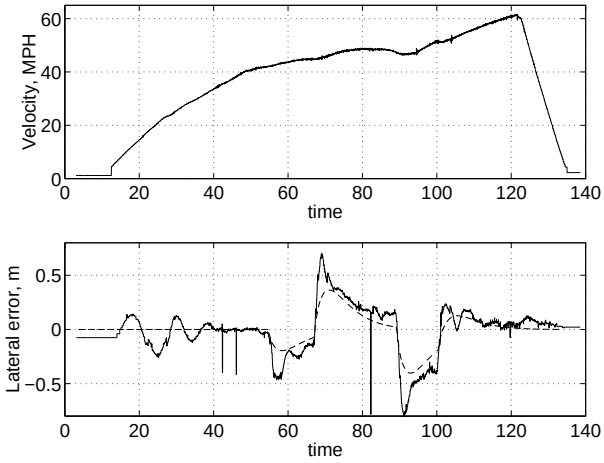

Figure 6.11: Velocity profile of the vehicle and lateral tracking error (time in sec) with robust H_∞ controller

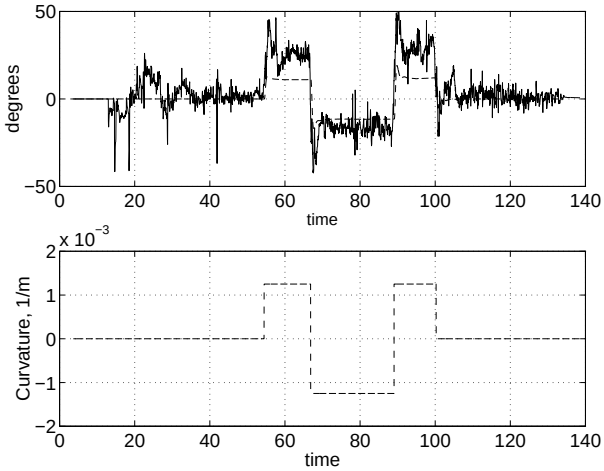

Figure 6.12: Steering wheel action and road curvature profile used in the simulation (time in sec) with robust H_∞ controller

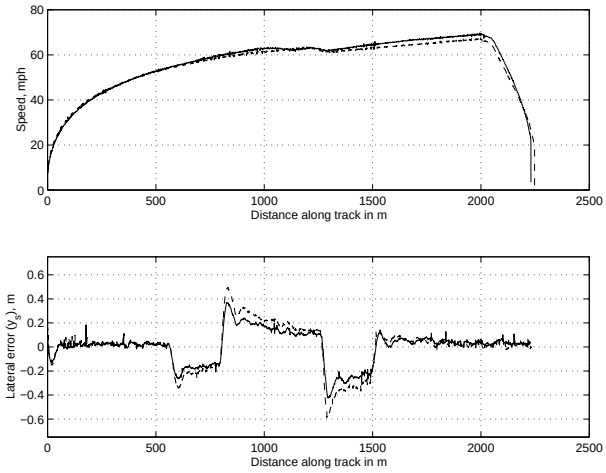

Figure 6.13: High speed tests with and without geometric feed-forward

Nevertheless, the match indicates usefulness of the simplified model.

Remarks

• In the present design, road information was not used. This information, when incorporated as a feed-forward, reduces the transient error. To show this, a geometric feed forwards term ($\delta_{feed\ forward} = (l_1 + l_2)\rho$ as in Hingwe, 1997) was added. The comparison between the feed-forward and no feed-forward case is shown in Figure 13 . For comparison, the velocity and the lateral errors are plotted against absolute position of the vehicle on the test track. Dashed line represents LPV controller without feed-forward term and the solid line represents the closed loop results with LPV+feed-forward term. The transient error at curve transitions has decreased by .075 m but the closed loop dynamics have remained unaffected as expected.

• Only the lateral error measured at the front bumper was used in feedback control. Use of relative yaw (by using measurements from sensor at the rear of the tractor) will result in an easier control problem, hopefully allowing to improve either the performance and/or increasing the speed of operation.

• Stability of the yaw internal dynamics was not directly addressed in the control synthesis. However, the smoothness requirement on the steering action and low frequency tracking requirement eliminate excitation of the yaw dynamics oscillation. One way of explicitly adding this requirement in the design is by including relative yaw and articulation angle in the definition of "error". Appropriate frequency dependent weight on these quantities will eliminate such controllers which may cause excitation of the yaw dynamics.

• The robustness of the control design to parametric uncertainties like the mass and cornering stiffness was not addressed. This may be addressed by including iteration for robustness much in the way robustness is incorporated in the μ synthesis techniques. However, this is a direction of future research effort.

To show that LTI designs for a fixed velocity are not adequate at other velocities, LTI controllers at fixed velocities (20, 40 and 60 MPH) with identical weighting functions and problem formulation as in LPV design were designed. Figure 14 shows the closed loop results for H_∞ controller designed for 40 MPH. It can be seen that the performance at 20 MPH and at 60 MPH is worse than performance at 40MPH.

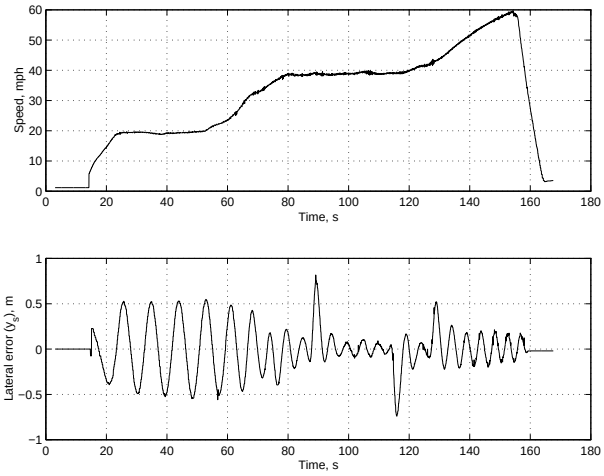

Figure 6.14: Closed loop results for H_∞ controller designed at 40 MPH

6.8 Conclusions

It is known that the linearized lateral dynamics of tractor semi-trailer vehicle are dependent on the longitudinal velocity. This warrants a velocity dependent lateral controller. LPV based controller design is one way to incorporate velocity dependence in the controller. A controller which sought appropriate tradeoff between tracking and steering effort was designed. The controller was tested in closed loop on a class eight tractor semi-trailer vehicle at speeds up to 65 mph. For comparison, an identical problem formulation was used to design an optimal H_∞ controller at fixed nominal velocity but robust to a range of velocities. This controller worked for changes in velocity as well but the performance was poorer. The fact that the LPV controller works well in experiments suggests that (i) the linearized model captures significant dynamics of the vehicle and (ii) the design tools in frequency domain can be quite intuitive and powerful. For vehicle control application, the LPV approach is probably the least conservative of the commonly used linear design tools and therefore gives a better performance.

Chapter 7

Conclusions

In this report five lateral control methodologies for tractor-semitrailers were presented. It was shown that the problem of steering control of tractor semitrailers is complicated by nonlinerities because of vehicle longitudinal speed and tire model. However, it is possible to linearize the model and design controllers around a nominal operating point (fixed space and small steering and articulation angle). Robust H_∞ controller was the example of such a design. On the other hand it is possible to include all nonlinearities in the model and design a nonlinear controller. Robust Feedfack linearization controller and loop-spaded nonlinear controllers were examples of this strategy. These controllers rely on feedback from sensors for yaw rate, articulation angle and acceleration besides position feedback from magnetic markers and magnetometers. This makes the implementation complex in face of sensor noises and biases. In fact, the sensor noise and bias restricted experiments with these controllers to low speed (less than 35MPH).

The controllers designed with a linear model assumption (fixed velocity) have the advantage of using fairly sophisticated tools for optimal design which trades off robustness and performance criteria. These controllers relied on feedback from position sensors only. This measurement has more sensitivity and lower noise as compared to yaw rate and acceleration sensors. Thus these controllers exhibited smooth steering and were tested at 45-50 MPH. However, controllers designed for 60MPH did not exhibit good performance at low speeds and were marginally stable at high speeds (the phase lag in all vehicles increases at the vehicle speed increases).

In Chapter 5, we explained how LPV model (where vehicle speed is a measured parameter in the model) includes the dominant nonlinearity (longitudinal speed) while allowing control sysnthesis based on linear design tools. Experimental results showed that this may be a good compromise between linear time invarient controllers and nonlinear controllers.

LPV controller does not take into account robustnedss explicitly. However, limited testing indicated robustness to change in load. Another controller, gain scheduled H_∞ allows incororating robustness and performance metrics in the design explicitly. This controller was shown to work in simulations.

THe following table summarizes the highlights of each controller and provides comparitive characteristics.

The task items were addressed in the following manner:

- Task 4. Linear as well as nonlinear controllers were designed and simulated using the model parameters identified in previous studies. The simulations matched the experimen-

Table 7.1: Characteristics of steering controllers in the report

Controller	Performance	Robustness	Sensors used	ease of tuning
Nonlinear Loop Shaped	adequate at low speed	Explicitly modeled	lateral, yaw and articulation	Field tunable but difficult
Robust Feedback	Tested in simulation	Explicitly modeled	lateral, yaw and articulation	Field tunable but difficult
Robust H_∞	Good at designed speeds	Explicitly modeled	front and rear lateral sensors	Tuning done at performance weights
Gain Scheduled H_∞	Tested in simulation	Explicitly modeled	front and rear lateral sensors	Tuning done at performance weights
LPV Controller	Tested at high speed	Not modeled	Front lateral sensor	Tuning done at performance weights

tal data well (see Chapter 5, LPV controller expermintal results and Chapter 3, Robust H_∞ results).

- Task 5. Closed loop experiments were performed at speeds of 55 MPH (and upto 70 MPH) in Crow's Landing test site.

- Task 6. Observations from implementing the Robust H_∞ controller, loop-shaped controller, nonlinear sliding mode controller and LPV controller were used to comment on the range and sensitivity of actuators and sensors. It was concluded that the lateral position sensor range (+ - 0.8m) is adequate for class 8 tractor semitrailer. The maximum range consumed during experiments at 55 MPH was 0.5 m. The sensor noise was low enough to provide smooth steering action. The acceleration and yaw measurement was noisy and constrained the performance of the nonlinear sliding mode controller. However, they were successfully used for system identification and modeling.

- Task 7. LPV controller required that the acceleration and deceleration of the vehicle be within specified bounds for stability guarantee. The bounds choosen for the control design were such that they would allow extreme braking and pedal to the metal acceleration of nominally loaded semitriler. The conroller was tested in such situation (Chapter 5, experimental results with PV) and worked well. The present study indicated possible use of differential braking for yaw dynamics control (jack-knifing and fish-tailing) and that is proposed to be studied in MOU 385.

  A video of the tractor-trailer under automated operation has been produced and is available on request from PATH publications office or on web at
  www.path.berkeley.edu/PATH/publications/videos/auto-truck.ram

  The focus of this MOU was providing proof-of-concept of automated steering of tractor semi-trailes at highway speeds. This objective facilitated model assumptions like small articulation angle and small steering angle. Future work should perhaps focus on scenarios where articulation angle and steering angle is large. Such scenarior include jack-knifing and fish-tailing, small radius low speed turning, and backing the tractor-trailer.

Acknowledgement

This work was sponsored by California PATH program. The contents of this report reflect the views of the authors who are responsible for the facts and the accuracy of the data

presented herein. The contents do not necessarily reflect the official views or policies of the state of California. This report does not constitute a standard, specification, or regulation. Authors also acknowledge the technical contributions of H.S. Tan, B. Bougler, D. Nelson, P. Kretz and B. Prohaska.

Bibliography

[1] Chen, C. and Tomizuka M., "Steering and Independent Braking Control for Tractor-Semitrialer Vehicles in Automated Highway Systems", Proceedings of the 34th IEEE Conference on Decision and Control, 1995, New Orleans, Vol 2, pp 1561-1566

[2] Canudas de Wit, C., "Trends in Mobile Robot and Vehicle Control", Control Problems in Robotics and Automation, Springer Verlag, Germany, 1998.

[3] Fritz, H., "Longitudinal and Lateral Control of Heavy-Duty Trucks for Automated Following in Mixed Traffic: Experimental Results from Chauffeur Project", presented at the 1999 IEEE Conference for Decision and Control, Hawaii.

[4] Bruin, Dik de and Bosch, van Den, "Modeling and Control of Double Articulated Vehicle with Four Steering Axles", presented at the American Control Conference, San Diego, 1999, pp 3231-3235.

[5] Tai, M., and Tomizuka M., "Robust Lateral Control of Heavy Vehicles for AHS" presented at the 1999 IFAC Congress, Beijing, China.

[6] Hingwe, P., Tai M., Wang Y-Y and Tomizuka M., "Lateral Control of Tractor Semitrialer Vehicles for Automated Highway Systems: An Experimental Study", presented at the 1999 ASME IMECE, Nashville TN.

[7] Guldner, J., Sienel W., Tan H-S, Patwardhan S., Ackermann J. and Bunte T., "Robust Automatic Steering Control for Look Down Reference Systems with Front and Rear Sensors" IEEE Transactions on Control Systems Technology, Vol 7, No 7, pp 2-11 January 1999.

[8] Wu, F., "Control of Linear Parameter Varying Systems", PhD Dissertation, Department of Mechanical Engineering, UC Berkeley, CA May 1995.

[9] Feng, K.-T., Tan, H.-S. and Tomizuka, M, "Influence of Suspension Roll Dynamics on Vehicle Steering Control", to appear in IEEE/ASME transactions on mechatronics.

[10] Slotine, J.J., and Li, W., "Applied Nonlinear Control", Prentice Hall, 1991.

[11] Hingwe, P., and Tomizuka, M, "A variable Look-Ahead Controller for Lateral Guidance of Four wheeled Vehicles", presented in the American Control Conference, 1998, pp 31-35.

[12] Peng, H. and Tomizuka, M., 1993, "Preview Control for Vehicle Lateral Guidance in Highway Automation," *ASME Journal of Dynamic Systems, Measurement and Control*, Vol. 115, No. 4, pp. 678-686.

[13] Wu, F., Yang X. H., Packard A. and Becker G., "Induced $\mathcal{L}_2$ Norm Control for LPV Systems with Bounded Parameter Rate", I. J. of Nonlinear and Robust Control, Dec 1996.

[14] Shamma, J. and Athans M., "Gain Scheduling: Potential Hazards and Possible Remedies" IEEE Control Systems Magazine, vol 12, pp. 101-107, 1992

[15] Shahruz, S. and Behtash S., "Design of Controllers for Linear Parameter Varying Systems by the Gain Scheduling Technique", J. of Mathematical Analysis and Applications, vol 168, pp. 195-217, 1992.

[16] Boyd, S., Ghaoui, L. El, Feron, E., and Balakrishnan, E., "Linear Matrix Inequalities in System and Control Theory", SIAM studies in Applied Mathematics, vol 15, 1994.

[17] Tomizuka, M., M. Tai, J-Y. Wang and P. Hingwe, (1999). "Automated Lane Guidance of Commercial Vehicles," Proceedings of the 1999 IEEE International Conference of Control Applications, pp. 1359-1364, Hawaii, August 1999.

[18] Tai, M and M. Tomizuka, (1999). "Robust Lateral Control of Heavy Duty Vehicles for Automated Highway Systems," Proceedings of the 14th IFAC World Congress, Vol. Q, pp. 37-42, Beijing, China, July 1999.

[19] Ackermann, J., J. Guldner, W. Sienel, R. Steinhauser, (1995). "Linear and Nonlinear Controller Design for Robust Automatic Steering," *IEEE Trans. on Control Systems Technology,*, Vol 3, pp. 132-143.

[20] Hingwe, P and M. Tomizuka, (1995). "Two Alternative Approaches to the Design of Lateral Controllers for Commuter Buses based on Sliding Mode Control," ASME International Mechanical Engineering Congress and Exposition, DSC-vol.56/DE-vol.86, pp.99-104.

[21] Krstic, M., I. Kanellakopoulos and P. V. Kokotovic, (1995). " Nonlinear and Adaptive Control Design," New York: Wiley.

[22] Tai, M. and M. Tomizuka, (1998). "Dynamic Modeling of Multi-Unit Heavy Vehicles," Proceeding of the 1998 International Mechanical Engineering Congress and Exposition, DSC-Vol. 64, pp. 673-680, Anaheim, November 1998.

[23] Hingwe, P., M. Tai and M. Tomizuka, (1999). "Modeling and Robust Control of Power Steering System of Heavy Vehicles for AHS," Proceedings of the 1999 IEEE International Conference of Control Applications, pp. 1365-1370, Hawaii, August 1999.

[24] Chen, C. and M. Tomizuka (1995). Steering and Independent Braking Control of Tractor-semitrailer Vehicle in Automated Highway Systems. Proc. of IEEE Conference on Decision and Control, New Orleans, 1561-1566.

[25] Hingwe, P., Packard, A. and Tomizuka, M. (2000),"Linear Parameter Varying Controller for Automatic Lane Guidance - Experimental Study on Tractor-Semitrailer Vehicle," submitted to the 2000 American Control Conference.

[26] Martin J.C. and G. Leitmann, (1981), "Continuous State Feedback Guaranteeing Uniform Ultimate Boundedness for Uncertain Dynamic Systems," IEEE Transactoins on Automatic Control, Vol. AC-26, No. 5, 1981.

[27] Fenton, R. E. and R. J. Mayhan (1991), " Automated Highway Studies at Ohio State University-An Overview," IEEE Transactions on Vehicular Technology, Vol. VT-40, No. 1, pp. 100-113.

[28] Shladover, S. et al. (1991), " Automatic Vehicle Control Development in PATH Program," IEEE Transactions on Vehicular Technology, Vol. VT-40, No. 1, 114-130.

[29] C. Chen and M. Tomizuka, "Dynamic Modeling of Articulated Vehicles for Automated Highway Systems", *Proc. of American Control Conference, Seattle*, pp. 653-657, 1995.

[30] M. Tai and M. Tomizuka, "Dynamic Modeling of Multi-Unit Heavy Vehicles", *International Mechanical Engineering Congress & Exposition*, Anaheim, pp.673-680, 1998.

[31] D. McFarlane and K. Glover, "Robust Control Design Using Normalized Coprime Factor Plant Description", *vol.138 of Lecture Notes in Control and Information Sciences*, Spring-Verlag, 1989.

[32] J.-Y. Wang, and M. Tomizuka, "Analysis and Controller Design Based on Linear Model for Heavy-Duty Vehicles", *International Mechanical Engineering Congress & Exposition*, Anaheim, pp.729-735, 1998.

[33] P. Hingwe, "Robustness and Performance Issues in the Lateral Control of Vehicles in Automated Highway Systems", PhD thesis, University of California at Berkeley, 1997.

[34] J. Sefton and K. Glover, "Pole-Zero Cancellations in the general H_∞ problem with reference to a two block design", *Syst. Contr. Lett.*, vol.14, pp.295-306, Apr. 1990.

[35] M. Tsai, E. Geddes and I. Postlethwaite K, "Pole-Zero Cancellations and Closed-Loop Properties of An H_∞ Mixed Sensitivity Design Problem", *Automatica* 3:519-530, 1992.

[36] R. A. Hyde, "The Application of Robust Control to VSTOL Aircraft", PhD thesis, University of Cambridge, 1991.

[37] I. Postlethwaite and D. J. Walker, "Advanced Control of High Performance Rotorcraft", Institute of Mathematics and Its Applications Conference on Aerospace Vehicle Dynamics and Control, Cranfield Institute of Technology, pp.615-619, 1992.

[38] M. Fujita, K. Hatake, F. Matsumura and K. Uchida, "Experiments on the Loop Shaping Based H_∞ Control of a Magnetic Bearing", *Proc. of American Control Conference*, San Francisco, pp.8-12, 1993.

[39] S. Mammar, "H_∞ Robust Automatic Steering of a Vehicle", *Proc. of IEEE Intelligent Vehicle Symposium*, Piscataway, NJ, pp.19-24, 1996.

[40] R.T. O'Brien, P. A. Iglesias, and T. J. Urban, "Vehicle Lateral Control for Automated Highway System", *IEEE Trans. on Control System Technology*, vol.4, no.3, pp.266-273, 1996.

[41] K.V. Fernando and H. Nicholson, "Singular Perturbational Model Reduction of Balanced Systems", *IEEE Trans. on Automatic Control* AC-27(2):466-468, 1982.

[42] J.-Y. Wang and M. Tomizuka, "Robust H_∞ Lateral Control for Heavy-Duty Vehicles in Automated Highway System", *Proc. of American Control Conference, San Diego, CA*, pp. 3671-3675, 1999.

[43] P. Hingwe, M. Tai, J.-Y. Wang and M. Tomizuka, "Lateral Control of Tractor-Semitrailer Combination for Automated Highway Systems–An Experimental Study", *International Mechanical Engineering Congress & Exposition, ASME Symposium on Transportation Systems*, 1999.

[44] S. Patwardhan, H.-S. Tan, and J. Guldner, "A general Framework for Automatic Steering Control: System Analysis", *Proc. of American Control Conference*, Albuquerque, New Mexico, pp.1598-1602, 1997.

[45] S. Mammar, "Robust Reduced Order Two-Degree-of-Freedom Tractor-Semitrailer Lateral Control", *Proc. of American Control Conference, San Diego, CA*, pp. 3158-3162, 1999.

[46] P. Kapasouris, "Gain-Scheduled Multivariable Control for the GE-21 Turbofan Engine Using the LQG and LQG/LTR Methodology", Master's thesis, Massachusetts Institute of Technology, 1984.

[47] R.A. Hyde, "H_∞ Aerospace Control Design–A VSTOL Flight Application", Springer 1995.

[48] D.J. Stilwell and W.J. Rugh, "Interpolation of Observer State Feedback Controllers for Gain-Scheduling", *Proc. of American Control Conference, Philadelphia, PN*, pp. 1215-1219, 1998.

Appendix A

The inertia matrix M is

$$M = \begin{bmatrix} m_1+m_2 & -m_2(d_1+d_3) & -m_2d_3 \\ -m_2(d_1+d_3) & I_{z1}+I_{z2}+m_2(d_1+d_3)^2 & I_{z2}+m_2d_3(d_3+d_1) \\ -m_2d_3 & I_{z2}+m_2d_3(d_3+d_1) & I_{z2}+m_2d_3^2 \end{bmatrix}$$

The damping matrix D is

$$D = \frac{2}{v}\begin{bmatrix} C_{\alpha_f}+C_{\alpha_r}+C_{\alpha_t} & l_1C_{\alpha_f}-l_2C_{\alpha_r}-(l_3+d_1)C_{\alpha_t} & -l_3C_{\alpha_t} \\ l_1C_{\alpha_f}-l_2C_{\alpha_r}-(l_3+d_1)C_{\alpha_t} & l_1^2C_{\alpha_f}+l_2^2C_{\alpha_r}+(l_3+d_1)^2C_{\alpha_t} & l_3(l_3+d_1)C_{\alpha_t} \\ -l_3C_{\alpha_t} & l_3(l_3+d_1)C_{\alpha_t} & l_3^2C_{\alpha_t} \end{bmatrix}$$

The stiffness matrix K is

$$\bar{K} = 2\begin{bmatrix} 0 & -(C_{\alpha_f}+C_{\alpha_r}+C_{\alpha_t}) & -C_{\alpha_f} \\ 0 & -(l_1C_{\alpha_f}-l_2C_{\alpha_r}-(l_3+d_1)C_{\alpha_t}) & (l_3+d_1)C_{\alpha_t} \\ 0 & l_3C_{\alpha_t} & l_3C_{\alpha_t} \end{bmatrix}$$

The vectors F and E are

$$F = 2C_{\alpha_f}\begin{bmatrix} 1 \\ l_1 \\ 0 \end{bmatrix}$$

$$E = \begin{bmatrix} -2(l_1C_{\alpha f}-l_2C_{\alpha r}-(l_3+d_1)C_{\alpha t})-(m_1+m_2)v^2 \\ -2(l_1^2C_{\alpha f}+l_2^2C_{\alpha r}+(l_3+d_1)^2C_{\alpha t})+m_2(d_1+d_3)v^2 \\ -2(l_3(l_3+d_1)C_{\alpha t})+m_2d_3v^2 \end{bmatrix}$$